Carbon Monoxide Modulates the Innate Immune Response to Bacterial Lung Infection

Carbon Monoxide Modulates the Innate Immune Response to Bacterial Lung Infection

Ghee Rye Lee

A Thesis Submitted to the Faculty of

The Harvard Medical School

in Partial Fulfillment of the Requirements

for the Degree of Master of Medical Sciences in Immunology

Harvard University

Boston, Massachusetts.

May, 2018

Thesis Advisor: Dr. Leo Otterbein Ghee Rye Lee

Carbon Monoxide Modulates the Innate Immune Response to Bacterial Lung Infection

Abstract

Carbon monoxide (CO) is generated endogenously in all mammalian cells by the enzyme Heme Oxygenase-1 (HO-1). HO-1 is primarily responsible for heme metabolism but is also vital for the host's ability to appropriately respond to stress. While previously thought to be a functionless byproduct, CO is now accepted as possessing critical physiological and therapeutic properties at low concentrations. Treatment with low doses of exogenously-delivered inhaled CO (250 ppm; 0.025%) for as little as 1h confers protection in preclinical animal models of acute lung injury, ischemia/reperfusion injury, sepsis and organ transplantation. While the mechanism(s) of protection are poorly understood, studies indicate that CO modulates inflammation and regulates innate immune responses. We tested the hypothesis that exposure to CO would enhance bacterial clearance in a mouse pneumonia model and that the mechanism involves in part changes in macrophage and neutrophil phenotypes that become more effective at killing bacteria.

Employing a mouse model of bacterial pneumonia, we show that CO augments bacterial clearance in the lung airway at 24hr in CO versus air-treated animals. Cells that were collected from the airway by bronchoalveolar lavage were analyzed for phenotypic changes using CyTOF, a multi-dimensional single cell analysis tool. CO treated, infected mice showed unique populations of cells that were not observed in controls, including significant numbers of $CD68^{+}$ neutrophils and macrophages that expressed higher TLR2 and CD64 levels compared to control and may explain the enhanced bacterial killing. Collectively, my results demonstrate that CO augments bacterial clearance from the lung and does so in part by modulating immune cell

function. Future studies will examine how these particular cell populations contribute to protection against bacterial lung infection.

Table of Contents

Figures

Chapter 1: Background

Chapter 2: Data and Methods

Tables

Chapter 2: Data and Methods

Acknowledgements

I would like to thank each and everyone who helped me in any way throughout my time at Harvard Medical School and supported me to complete the research work.

First and foremost, I would like to express my sincerest gratitude to my thesis advisor Dr. Leo Otterbein for the patient guidance, untiring mentorship, heartfelt encouragement, and his vast knowledge and expertise in physiology and immunology. He has always been supportive of me since the day I joined his lab and he constantly inspired and challenged me to become an independent researcher, critical thinker, and creative scientist. My lab experience at the University of Pittsburgh Medical Center under the guidance of Dr. Edith Tzeng during my undergraduate time at Carnegie Mellon University sparked my interest in studying CO as a potential therapeutic agent and immunology and it means a great deal to me that I continued to study CO under Dr. Leo Otterbein who pioneered this field of study.

I also wish to thank Dave Gallo for helping me when working with lab animals and providing me with technical assistance and guidance in the lab. I am also grateful for his support during the times I encountered obstacles in research. In addition, I wish to extend my gratitude to the collaborators from Dr. Jim Lederer's lab at Brigham Women's Hospital, especially Josh Keegan and Laura Cahill for their assistance with CyTOF data analysis.

Special thanks to my colleagues, Dr. Mahtab Fahkari, Dr. Rodrigo Alves, James Harbison, Sherrie Otterbein and Dr. Shahzad Shaefi for lending me their expertise in lab work that provided solutions to any my scientific and technical problems arose during my research.

Last, but not least, I would like to thank Dr. Shiv Pillai, Dr. Michael Carroll, Dr. Diane Lam, Selina Sarmiento and the students of the MMSc in Immunology Program. I would not have been able to complete this program without their teaching, guidance and support.

"This work was conducted with support from Students in the Master of Medical Sciences in Immunology program of Harvard Medical School. The content is solely the responsibility of the authors and does not necessarily represent the official views of Harvard University and its affiliated academic health care centers."

Chapter 1: Background

1.1 Background

Carbon monoxide (CO) is a colorless, odorless and tasteless gas that is toxic at high doses released during combustion. The fact that CO is toxic at certain concentrations is expected because all substances are toxic to the body at certain exposure levels and CO is no different. CO has long been known as a "silent killer" due to its 250-fold higher affinity for hemoglobin (Hb) than oxygen, which compromises Hb's ability to deliver oxygen to tissues resulting in tissue hypoxia and asphyxiation[1]. In addition, CO binding to Hb stabilizes Hb's relaxed state and this carboxyhemoglobin complex exhibits higher affinity for oxygen, thus further reducing oxygen release into the tissue[2]. An inert, stable gas, CO is not metabolized and the elimination of CO can only be achieved by exhalation in the lung[3]. CO is also toxic to organisms because it interferes with mitochondrial respiration. It competes with oxygen for binding to ferrous heme a_3 of cytochrome *c* oxidase (COX), the last complex in the mitochondrial electron transport chain. By binding to COX, which interferes with electron transport, CO increases generation of reactive oxygen species[4].

This notorious reputation of CO, however, started to change in the 1960's, when it was recognized that CO is endogenously synthesized in all cells during the metabolism of heme by the ubiquitous enzyme heme oxygenase (HO)[5]. HO catalyzes the first step in heme degradation yielding biliverdin, iron and CO (**Figure 1**)[6]. Biliverdin is converted to

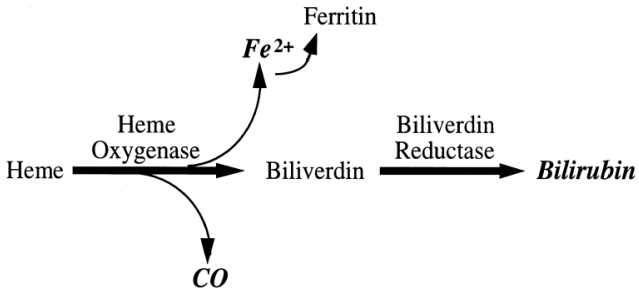

Figure 1. Heme metabolism by HO-1. As HO-1 breaks down heme, CO, Fe^{2+} and biliverdin are released in equimolar amounts. Fe^{2+} is rapidly sequestered into ferritin and biliverdin is converted into bilirubin by the enzyme biliverdin reductase.

bilirubin by biliverdin reductase and iron is rapidly sequestered into a ferritin. There are two isoforms of HO, HO-1 and HO-2, both of which catalyze the first and rate-limiting step in the degradation of heme. HO-1 is localized primarily in the endoplasmic reticulum and is found in all cells, especially those involved in erythrocyte and hemoglobin turnover such as the spleen, kidney, macrophages, and liver parenchyma[7]. While HO-1 is inducible by a large number of environmental agents other than heme, HO-2 is constitutively expressed primarily in the brain, vasculature, liver, kidney and testes[7].

Heme, the substrate of the enzyme HO, a porphyrin coordination complex that is comprised of a heterocyclic organic ring called porphyrin and a ferrous iron (Fe^{2+}) at the center. Porphyrins are formed by the linkage of four pyrrole rings through methyne bridges. The central metal ion binds to the nitrogen atom of each of the four pyrrole rings. The metal ion in hemoproteins serves as a physiologically important moiety in mammalian organisms. For example, oxygen binds to Fe^{2+} in hemoglobin and myoglobin and these hemoproteins function to transport oxygen in the blood and store oxygen in the muscle, respectively. Another example is cytochrome c, whose heme group accepts electrons from coenzyme Q and transfers them to Complex IV in the electron transport chain in mitochondria[3,8].

Heme synthesis is primarily carried out in erythroid precursor cells in the bone marrow and in hepatocytes. Heme is synthesized from the amino acid glycine and succinyl-CoA derived from the citric acid cycle, and it is catalyzed by the enzyme mitochondrial D-aminolevulinate (ALA) synthase. While the rate of heme synthesis is constant and stable in the bone marrow, the ALA synthase activity in the liver is largely influenced by the availability of heme, which acts as a negative regulator[8].

Heme degradation is occurs continuously in the body. Erythrocytes have a lifespan of approximately 120 days and the worn-out, senescent red blood cells are phagocytosed by macrophages in the spleen and liver, a process called erythrophagocytosis[8]. Macrophages also degrade the Hbs of the phagocytosed erythrocytes[8]. During erythrophagocytosis, studies showed that Hrg1, localized in endocytic compartments in macrophages, transports heme across the phagolysosomal membrane into the cytoplasm by passive diffusion[9,10]. Since HO is not present on the phagolysosomal membrane, degradation of heme by HO takes place in the cytoplasm[10].

In addition to breaking down heme, HO-1 is vital for the host's response to stress and homeostatic maintenance of cells and tissues after injury. In addition to heme, numerous stress signals and conditions can increase HO-1 expression, including trauma, hypoxia, hyperoxia, cytokines, pathogens, damage-associated molecular patterns and pathogen-associated molecular patterns[4]. Studies have demonstrated that greater induction of HO-1 leads to better survival in various *in vivo* models of tissue injury and cellular damage[11,12,13,14,15]. Importantly, lack of HO-1 is highly detrimental to the host. HO-1 deficient mice exhibit heightened susceptibility to stress from bacterial infection and ischemia reperfusion injury[16]. Likewise, human HO-1 deficiency showed similar hypersusceptibility to stress observed in HO-1 deficient mice with increased inflammatory indices including leukocytosis and thrombocytosis[17].

In the absence of HO-1, heme cannot be degraded efficiently and as a result, heme accumulates where it becomes highly toxic to the host. Heme itself induces reactive oxygen species production both through enzymatic reactions that involve NADPH oxidase and also through non-enzymatic reactions by converting organic hydroperoxides into free radicals[18]. Heme is also considered a damage-associated molecular pattern (DAMP) molecule because it exerts proinflammatory effects. Heme specifically binds to TLR4 on macrophages and

endothelial cells, resulting in the activation of the TLR4 signaling cascade that leads to intracellular oxidative stress and proinflammatory responses. Heme also increases endothelial permeability by inducing the expression of adhesion molecules such as ICAM-1 (intercellular adhesion molecule 1), VCAM-1 (vascular cell adhesion molecule 1), E-selectin and P-selectin, and thus facilitating the migration of neutrophils into tissues and triggering inflammation[62]. In healthy individuals and animals, excessive inflammation, and tissue injury by heme is not usually observed because HO-1 continuously degrades heme. However, prolonged exposure to excess heme as a result of HO-1 deficiency is detrimental to the host because heme will bind to TLR4 and exaggerate cell activation and death.

HO-1 expression and activation can quantitatively vary between individuals by the presence of a (GT)n microsatellite polymorphism in the promoter of the HO-1 gene, *HMOX1*[3]. Compared to a high number of (GT)n repeats, low frequency of repeats in the promoter region yields stronger HO-1 induction. Individuals with short (GT)n repeats are shown to be less prone to develop certain diseases such as emphysema[20], rheumatoid arthritis[21], and atherosclerosis[22]. These findings point to how indispensable HO-1 is in the host's ability to recover and survive from stress and injury is why HO-1 is now classified as a "protective gene"[23].

The mechanism by which HO-1 confers protection in the host is still not well understood. The data that has accumulated from many laboratories, including Dr. Otterbein's, suggest that the mechanism by which HO-1 imparts protection largely involves its ability to generate iron, biliverdin and CO. Each of these products influence cells via distinct molecular targets.

Iron

Ferrous iron (Fe^{2+}) can trigger upregulation of an iron-transporter channel that pumps iron out of the cell[24] and also induces expression of ferritin, preventing iron from contributing to the generation of ROS and further oxidative damage[25]. Ferritin is made of 24 subunits of two types: heavy chain, H-ferritin, and light chain, L-ferritin and H-ferritin is shown to have ferroxidase activity, converting ferrous iron to the ferric form (Fe^{3+}). Protective effect of H-ferritin has been characterized in the animal model of acute liver injury, where the transgenic mice with deletion of H-ferritin in proximal tubules are more susceptible to renal injury than wild-type littermates[7]. Additionally, H-ferritin has anti-apoptotic activity on endothelial cells and hepatocytes[57].

Biliverdin and Bilirubin

Biliverdin and bilirubin are both antioxidants but compared to biliverdin, bilirubin is a much more potent antioxidant because it has a superior ability to scavenge peroxynitrite-derived free radicals and superoxide derived from xanthine oxidase[26]. Bilirubin is also strongly antioxidant against almost 10,000-fold higher concentrations of H_2O_2[27]. Exogenous administration of biliverdin is shown to be bioactive and is protective in various inflammatory conditions including atherosclerosis and organ transplantation and it can substitute for the protection afforded by HO-1, when HO-1 is absent [28,29,30]. In addition to its antioxidant properties, anti-inflammatory properties of biliverdin have been reported in several studies. Biliverdin elicits anti-inflammatory effects by attenuating LPS-induced P- and E-selectin expression on endothelial cells, modulating the number of infiltrating neutrophils[31]. It was also reported that exogenous administration of biliverdin inhibited the upregulation of the pro-inflammatory cytokines IL-6, TNF and IL-1β[31,32]. Moreover, exogenous administration of

biliverdin was able to up-regulate the expression of the anti-apoptotic molecules Bcl-2 and Bag-1, independently of HO-1, in a model of ischemia/reperfusion injury[32]. Both bilirubin and biliverdin can exert cytoprotective effects alone; however, they can also impart protective effects through activation of biliverdin reductase, the enzyme that converts biliverdin to bilirubin. In macrophages, binding of biliverdin to biliverdin reductase activates PI3K-Akt signaling to increase the production of the anti-inflammatory cytokine IL-10[33]. Biliverdin reductase also acts as a transcriptional modulator. Binding of biliverdin to biliverdin reductase activates Ca^{2+}/CaMKK signaling that leads to phosphorylation of eNOS and the production of nitric oxide (NO). NO, in turn, nitrosylates biliverdin reductase, which enables its translocation to the nucleus where nuclear biliverdin reductase binds to the TLR4 promoter to inhibit its expression[34]. Further, lack of biliverdin reductase in macrophages results in an amplified pro-inflammatory phenotype with increased TNF and TLR4 expression[34].

Carbon Monoxide

Carbon monoxide (CO) at low concentrations possesses many important physiological and salutary properties[3]. Studies have shown that exogenous administration of CO can rescue animals deficient in HO-1 and, as such, mimic the beneficial effects of HO-1 induction[35,36]. Exposing animals to exogenous CO at 250ppm for as little as 1h provides remarkable protection in many preclinical animal models including organ transplantation[37], ischemia/reperfusion injury[38], shock (endotoxin/hemorrhagic/infection)[39,40,41], vascular injury[42,43,44], malaria[45], sepsis[46,47,48] and acute lung[49,50] and liver injury[51,52]. Thus it is not surprising that potential therapeutic effects of CO are currently being tested in clinical trials for paralytic ileus, pulmonary fibrosis, pulmonary hypertension and organ transplantation [www.clinicaltrials.gov].

Of the three products produced by HO-1, CO has been the most extensively studied in various animal models and it is the only one that has translated to clinical settings. Unlike iron or biliverdin, CO is non-reactive and non-metabolized. Moreover, the delivery method is straightforward because it is easily administered as an inhaled gas or as a CO–releasing molecule (CO-RM)[3]. Variations of CO-RMs have been designed, including CO-RM1, CO-RM2, CO-RM3, CO-RMA1, and they differ in chemical structures and metals used to control the kinetics of CO release and target specific tissues and signaling pathways. For example, CO-RM3 can release CO rapidly and thus elicit a prompt vasodilatory response in a cGMP-dependent and endothelium-dependent way[53] while CO-RMA1, which releases CO relatively slowly, induces mild vasodilation in a potassium-channel-dependent and endothelium-independent manner[54]. CO can also be administered as a Hb saturated with CO, known as MP4CO, and more recently as a CO-saturated liquid. MP4CO was prepared in solution by conjugating polyethylene glycol to Hb saturated with 100% CO and when delivered intravenously, CO from MP4CO equilibrates with red blood cell Hb and exerts cytoprotective effects in myocardial infarction in rats and transgenic sickle cell anemia mice[55]. CO-saturated liquids can be prepared by saturating University of Wisconsin organ preservation solutions with CO (5%; CO-UW). *Ex vivo* treatment of intestinal grafts with CO-UW ameliorates intestinal transplant-induced ischemia/reperfusion injury[56]. Currently, HBI-002, a CO-saturated liquid formulation that is designed to be delivered orally, is being studied in kidney transplant to prevent delayed graft function and also in sickle cell disease to alleviate vasoocclusive crises. (http://www.hillhurstbio.com/hbi-002/).

That CO is a beneficial is no longer a question. The majority of efforts in labs around the world are now looking to understand how it functions in any given situation. CO can be pro-or anti-inflammatory, pro- or anti-apoptotic and pro- or anti-proliferative depending on the

circumstances and status of the cell and tissue (**Figures 2 & 3**). For instance, if CO is delivered after bacterial challenge, CO imparts pro-inflammatory effects by boosting macrophage phagocytosis, bacterial clearance and reducing heme bioavailability[23]. By contrast, when it is delivered before an inflammatory stimulation, CO can be anti-inflammatory by modulating the activity of peroxisome proliferator-activated receptor -γ (PPARγ)[58] and hypoxia-inducible factor 1α (HIF1α)[59], increasing the ROS and lysosome generation and inducing the expression of the anti-inflammatory gene IL-10 in macrophages (**Figure 3**)[60]. Different components of the vasculature respond to the CO treatment differently as well. For example, CO is pro-proliferative for endothelial cells and anti-proliferative for vascular smooth muscle cells. Treatment with CO enhances endothelial cell proliferation by activating the small G protein RhoA, accelerating cellular entry into S phase and phosphorylation of Rb, and resulting in enhanced proliferation of endothelial cells[61]. On the other hand, CO suppresses proliferation of vascular smooth muscle cells by inhibiting intimal hyperplasia in an animal model of balloon angioplasty[62]. CO can exert pro- or anti-apoptotic effects. For example, exposure to CO prevents endothelial cells from undergoing apoptosis and the mechanism involves activation of p38 mitogen-activated protein kinase (MAPK) signal transduction pathway[63]. However, CO has pro-apoptotic effect on Jurkat cells, a human T lymphocyte cell line. CO enhances Fas/CD95-induced cell death in T cells by up-regulating the pro-apoptotic protein FADD and activating caspase-8,9, and 3 while down-regulating the anti-apoptotic protein Bcl-2[64]. These findings suggest that under certain inflammatory or disease conditions, CO can exhibit different properties and target different cells in a manner that optimizes survival of the host and recovery of damaged tissues and cells.

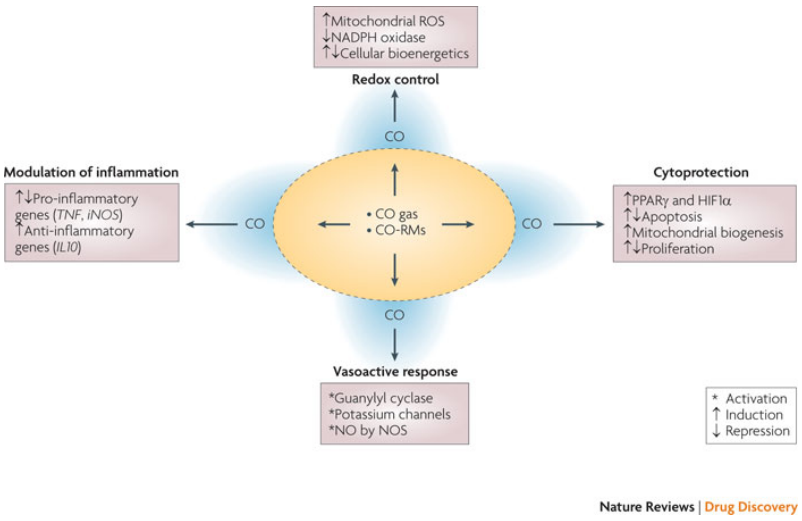

Figure 2. Therapeutic properties of CO gas[3]. Potential beneficial effects of CO in animal models of disease and injury occur through various cellular and molecular mechanisms of action that include redox control, cytoprotection, vasoprotection and modulation of inflammatory response.

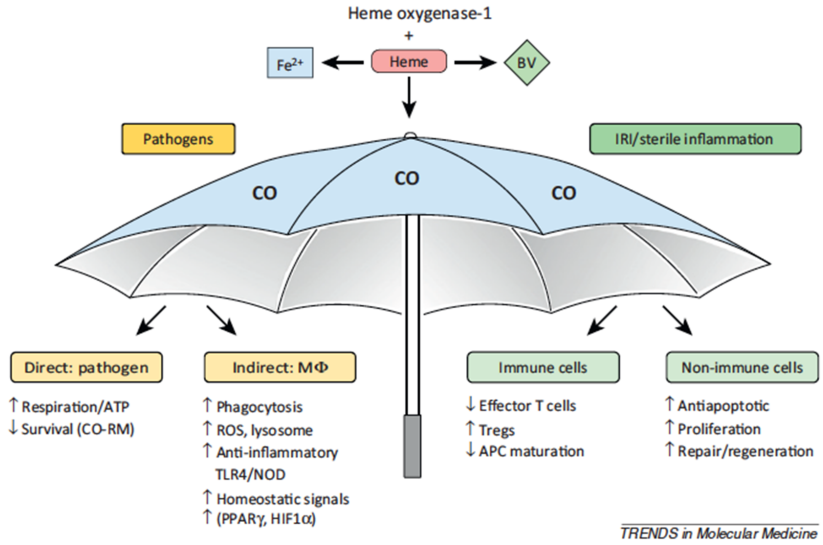

Figure 3. HO-1 and CO in immune responses[23]. Induction of HO-1 and exogenous administration of CO gas can exert salutary effects against pathogenic and sterile inflammatory conditions by regulating different aspects and cells of the innate immune response to stressors. HO-1/CO can augment the macrophages' ability to fight against the pathogens by augmenting phagocytosis, ROS, lysosome generation, and modulating TLR4/NOD signaling pathway to produce anti-inflammatory effect. Under sterile inflammatory condition, HO-1/CO inhibits proliferation and activation of effector T cells but promotes expansion of regulatory T cells (Tregs). It can also enhance anti-apoptosis and proliferation of endothelial cells[23]. (Abbreviations: BV, biliverdin; IRI, ischemia-reperfusion injury; APC, antigen presenting cell)

Dr. Otterbein's laboratory and other collaborating laboratories have established that HO-1 plays a protective role and that CO treatment is effective at bacterial killing in peritonitis models[65]. However, whether a similar effect exists in bacterial pneumonia has not been explored.

Differences between peritonitis and pneumonia include specific bacteria that might be involved and the relative oxygen concentration differences between the airway and the peritoneum.

Pneumonia is a bacterial and/or viral infection of the lung tissue and the World Health Organization estimates that lower respiratory tract infection is the most common infectious cause of mortality, resulting in 3.2 million deaths worldwide in 2015[66]. Bacterial pneumonia can either be community-acquired or hospital-acquired. Community-acquired pneumonia can be caused by antibiotic-sensitive strains of bacteria such as *Streptococcus pneumoniae* and, *Chlamydia pneumoniae*. By contrast, hospital-acquired pneumonia, which is one of the most common nosocomial infections, is caused by antibiotic-resistant strains of *Staphylococcus aureus* and *Pseudomonas aeruginosa*[67]. While anyone can develop pneumonia certain groups are at higher risk. For example, elderly, young children, individuals with chronic health problems, and hospitalized patients who became immunocompromised are more susceptible to opportunistic infections. The emergence of antibiotic-resistant strains of bacteria makes the treatment of pneumonia increasingly difficult, especially in immunocompromised individuals. Questions still remain regarding the etiologies of pneumonia, especially in specific age groups of people and patients who are at higher risk. Additionally, the emergence of antibiotic-resistance requires that more research is needed to develop effective therapeutic interventions for bacterial killing and protection of the host.

In this study, we tested whether CO treatment would augment the hosts ability to clear bacteria in the lung. Our central hypothesis is that: ***CO impacts bacterial clearance by modulating the phenotype of alveolar macrophages and neutrophil recruitment***. To test this hypothesis, we examined the phenotypic changes of alveolar macrophages and recruited neutrophils using a sophisticated approach with a multi-dimensional single cell analysis tool

called CyTOF which is a hybrid between a mass spectrometer and flow cytometer. Further, we explored how the lack of either alveolar macrophages or neutrophils affects the hosts ability to fight against lung infection and examined whether CO treatment in such settings would continue to benefit the host.

Chapter 2: Data and Methods

2.1 Introduction

In order to test the hypothesis that inhaled CO treatment augments the hosts ability to clear bacteria in the lung, we first established a mouse pneumonia model. A detailed design of this model is shown in section *2.1.1.* In this project, *Staphylococcus aureus* was used since it is a common Gram-positive bacteria strain found in early post-traumatic pneumonia. A dose response was first performed to determine the optimal amount of bacteria to elicit an inflammatory response. Animals were treated with or without CO (250 ppm for 1h) in the presence of bacteria. The model was designed with clinical relevance in mind so CO was begun 4h after bacterial inoculation into the lungs. A bronchoalveolar lavage (BAL) was performed at different time points to harvest cells, proteins, tissue, as well as bacteria as relevant readouts and endpoints. Male CD-1 outbred mice were used at a weight range of 25-30g and all procedures were approved by the BIDMC Institutional Animal Care and Use Committee.

Macrophages and neutrophils are the two major innate immune cells that are involved in inflammation caused by microbial invasion of the host. In healthy mice, airway leukocytes consist of approximately 95% alveolar macrophages, 1-4% lymphocytes and 1% neutrophils[68]. Alveolar macrophages serve as the front line of defense against respiratory particulates and microbes and their primary role is to ingest inert particulates without triggering inflammatory responses[68]. However, in the case of pathogen invasion, innate immune responses are triggered, where macrophages phagocytose microbes and produce pro-inflammatory cytokines, notably IL-8 and related CXC chemokines to recruit circulating neutrophils from the lung capillary networks into the airway[68]. In addition, alveolar macrophages produce CC chemokines including MCP-1 and RANTES to recruit circulating monocytes and lymphocytes into the airway[68]. In our

model of pneumonia, it took more than one hour for neutrophils to arrive in the airway after infection. A significant number of neutrophils were observed 4 hours and 24 hours after bacterial infection. Five hours after bacterial inoculation, macrophages and neutrophils were the majority of BAL cells present (**Figure 11**). Based on the known functions of macrophages and neutrophils in response to microbial infection and our data showing they are the majority of cells present in the BAL after infection, we hypothesized that the elimination of alveolar macrophages or neutrophils in the lung would weaken the host's ability to clear bacteria in the lung. In order to test this hypothesis, clodronate liposomes were used to deplete alveolar macrophages and the host's response to bacterial lung infection was assessed. Empty liposomes were used as a control. In order to deplete neutrophils, anti-Ly6G antibody was given to the animals because Ly6G is a neutrophil specific marker and other studies reported that neutrophils are successfully depleted by using this antibody[69]. Whether CO's ability to enhance bacterial clearance in the lung is mediated through neutrophils was tested by giving inhaled CO treatment to neutrophil-depleted mice.

We were interested in detailing the phenotypes of cells that responded to the bacterial challenge including the resident alveolar macrophages and the rapid infiltration of neutrophils and how these would be altered in response to CO. To do this, we used the advanced multi-dimensional single-cell analysis tool called CyTOF. CyTOF is a combination of mass spectroscopy and flow cytometry, termed mass cytometry. Instead of using fluorophores as detection reagents, which are used in flow cytometry, CyTOF exploits heavy metal isotopes. Heavy metal isotopes offer advantages over fluorescence-based applications because mass cytometry can detect discrete peaks of each metal isotope without significant overlap, thus

allowing users to detect up to 40 markers on the cells of interest simultaneously with greater sensitivity. Flow cytometry can use up to 12 markers and a panel of antibodies with conjugated fluorophores needs to be designed carefully in order to avoid the overlap in excitation and emission spectra. In this CyTOF experiment, we selected markers that are well characterized in innate immune cells. Data collected by CyTOF staining is analyzed with the aid of sophisticated software called cytobank (www.cytobank.org). The analysis tool from cytobank we used is viSNE, a visualization tool for high-dimensional signle-cell data based on the t-Distributed Stochastic Neighbor Embedding (t-SNE) algorithm. This tool generates a *viSNE map* where each cell is located in relation to another based on their similarity in phenotypic markers, enabling us to identify subsets of immune cells[71].

2.2 Materials and Methods

2.2.1 Mouse Pneumonia Model

(1) Bacteria Growth

Staphylococcus aureus (S. aureus) was grown in 100ml Tryptic Soy Broth (BD 25923) in a 37°C incubator shaker overnight to reach the stationary phase. Next, 2 ml of the overnight culture was transferred into a fresh 100 mL tryptic soy broth and grown in a 37°C incubator shaker for 1.5 hrs to allow the bacteria to reach the log phase of growth. Log phase is characterized by the bacterial cells doubling at a constant rate and the purpose of having bacteria in the log phase is that when delivered to the animals, bacteria can effectively grow and infect the host. Bacteria were then transferred into 2. 50 ml conical tubes and centrifuged at 4000 rpm for 10 minutes at 4°C. The supernatant was discarded and the pellet was diluted with sterile saline accordingly to reach an optical density (OD) of 0.3 spectrophotometrically using a SpectraMax M5 plate reader with SoftMax Pro 5 software. 100ul of the bacterial culture was added to a well in a 96 well plate and the OD was measured at 600 nM absorbance wavelength and compared to 100ul of soy broth to account for background absorbance. The background OD of the plate was subtracted from the bacteria sample OD to determine the actual OD of the sample. This baseline bacteria culture was kept on ice at all times to prevent further growth. The OD of 0.3 was chosen because 80ul of the bacteria culture of 0.3 OD is equivalent to ~10^6-10^8 colony forming units as previously determined by the Otterbein laboratory that when given to mice elicits a reproducible and non-lethal inflammatory response.

(2) Bacteria Plating and counting

To determine how many bacteria are in a sample, 10 ul of baseline bacteria at 1:10,000 and 1:1,000,000 dilutions in sterile saline was streaked on to petri dishes on Tryptic Soy Agar (BD 90002), a growth medium that provides nutrients for microorganisms. After streaking, using sterile technique, the plates were placed in a 37°C incubator overnight inverted to determine the amount of bacteria present and importantly to be able to correlate with the OD of 0.3 determined the day before. Colony forming units (CFU) of bacteria were determined the next day by counting the individual number of colonies or groups of microbes formed on the plate. Each colony originated from a single bacteria growing through replication. CFU counting is a method of measuring how many viable microbes were present in the original sample. In this study, 10ul of bacteria at 1:10,000 dilutions yielded ~50 to 300 CFUs per plate while 10ul of bacteria at 1:1,000,000 dilutions yielded ~1 to 10 CFUs per plate.

(3) Intratracheal delivery of bacteria

Male CD-1 mice were weighed and anesthetized by intraperitoneal injection of ketamine (10mg/kg) and xylazine (4mg/kg). After ~5 minutes, the animals were assessed to see if they were sufficiently anesthetized, which was confirmed by checking: (1) a slowed breathing rate; (2) no movement when picked up; (3) no response when their paws are gently pinched. Mice were then positioned on an inclined platform. The tongue was carefully grasped using blunt-ended forceps to provide space for a 22G angiocatheter to be inserted into the trachea. 80 ul of bacteria (OD 0.3) was aerosolized into the angiocatheter with a 1cc syringe and the mice were kept inverted for at least 10 sec so ensure the bacteria were fully inhaled into the lungs. Mice were then placed on a heating pad for recovery until they become fully awake so as to minimize the loss of body heat because anesthetized mice are hypothermic.

(4) Bronchoalveolar Lavage (BAL)

Male CD-1 mice were weighed and anesthetized by intraperitoneal injection of ketamine (10mg/kg) and xylazine (4mg/kg). Mice were anesthetized as above before performing the BAL. A midline laparotomy was then performed. Liver, pancreas, stomach and intestines were gently pushed to one side to better visualize the aorta. The descending aorta was cut and the diaphragm was carefully punctured to avoid damaging the lungs. A midline incision was made on the neck. The glands and the muscles around the trachea were removed to better visualize and expose the trachea. A 22G angiocatheter was inserted between the rings of the trachea and tied with a 4-0 silk suture. 1 ml of PBS was then infused and aspirated. This lavage was repeated three times and all the BAL fluid was combined in one 15ml conical tube and kept on ice. Collected BAL was centrifuged at 1500 rpm for 10 minutes at 4°C. The supernatant, which contains bacteria, airway cells and proteins, was separated from the cell pellet. The cell pellet was resuspended in 500 uL of PBS and 50 uL of the resuspension was cyto-centrifuged on a slide and stained with the Protocol Hema 3 stain set to visualize cell morphology and to count macrophages and neutrophils. The supernatant was vortexed and 10 ul of the supernatant (1:1 and 1:10 dilution in PBS) was plated on tryptic soy agar plates for CFU count as above. The plates were placed in a 37°C incubator overnight and the number of CFU was counted the next day as detailed above.

2.2.2 *In vivo* CO treatment

Male CD-1 mice were placed inside the chamber and treated with air (control) or CO (0.025%, 250 ppm) in a gas-tight plexiglass chamber (52.8 cm x 28.8 cm x 28.8 cm) for 1h. Before being delivered into the chamber, CO at a concentration of 1% (10,000 ppm) in compressed air was

mixed with compressed air and flow into animal chamber was maintained at rate of 12 liters/min. This rate ensured that there was no accumulation of CO_2, which might otherwise negatively impact the experiment. A CO analyzer (Interscan) was used to measure CO levels continuously in the chambers. It took approximately 15 minutes to reach the CO level of 250ppm in the cage and once 250 ppm of CO is reached in the CO chamber, the CO treatment time started. The mice were placed in the chamber four hours after bacterial challenge to simulate clinical therapeutic scenarios and also because that was previously determined to be the earliest time point that CO showed enhanced bacterial clearance in this pneumonia model (2.2.1). BAL was performed at 5 or 24 hours in separate cohorts of mice after bacterial challenge.

2.2.3 *In vivo* depletion of alveolar macrophages

Clodronate Liposome (www.clodronateliposomes.com) are a well-known reagent used to deplete macrophages. Clodronate liposomes are artificial spheres of concentric phospholipid bilayers that encapsulate clodronate. Macrophages can engulf liposomes easily by phagocytosis and after disruption of the phospholipid bilayers, clodronate accumulates intracellularly which becomes toxic and macrophages undergo apoptosis once the amount of clodronate exceeds a threshold concentration. PBS liposomes that lack clodronate served as a control. Male CD-1 mice were weighed and anesthetized as above and an intratracheal instillation was performed as detailed above. 50 uL of clodronate (Batch# C13T0517 and C19T0617) or PBS liposomes (Batch# P18T0617) were intratracheally instilled. At the completion of instillation, the mice were maintained in the inclined position until they were observed to have no difficulties breathing. They were then placed on a heating pad for recovery. Liposomes were administered five and four days before lung bacterial challenge (2.2.1). Five hours after bacterial challenge, a

BAL was performed to count and differentiate cells and determine bacterial counts. Bacterial CFU was determined in each BAL as above. A cell count was determined by hemocytometer and expressed as cells/ml. 50 ul of the cell suspension was cyto-centrifuged onto a glass slide with a Cytospin and a Quick-Diff stain was performed to determine the relative percentages of macrophages and neutrophils by standard morphological features.

2.2.4. *In vivo* depletion of Ly6G+ neutrophils

Neutrophil depletion was achieved by injecting 250ug or 500ug 1A8 monoclonal antibody (anti-Ly6G; BioXcell Cat# BP0075-1; Lot# 5857-2/1015, 626716O1, 626717M2B) diluted in 200ul PBS, i.p. Control mice were injected i.p. with an equivalent amount of 2A3 isotype control antibody (Rat IgG2a; BioXcell Cat# BP0089; Lot# 654817M2). Injection took place 24 hours prior to bacterial challenge. To determine neutrophil depletion, 100uL of whole blood in heparin (100 units/ml; Sagent 25021;) was drawn from the tail of the mouse prior to antibody administration and then again 24 hours after the antibody treatment. Whole blood was sent to the Longwood Small Animal Imaging Core Facility for complete blood count (CBC). BAL for cell and bacteria counts was performed on each animal as above.

2.2.5 CyTOF

Lung immune cells were collected 5 hours after bacterial challenge (2.2.1) to determine the cell phenotypes present in the airway in the presence and absence of CO (2.2.2). The BAL cells were either prepared immediately for staining (starting from 2.2.5.3) or kept frozen (starting from 2.2.5.1) to be analyzed in the future. The cell-surface and intracellular CyTOF staining protocol with barcoding was graciously provided by the laboratory of Dr. Jim Lederer, BWH.

The panel of antibodies conjugated to heavy metal isotopes was designed based on the markers that are known to play a role in innate immunity (**Table 1**). These antibodies and heavy metal isotopes are designed and prepared by the laboratory of Dr. Jim Lederer, BWH.

(1) Cell Freezing and Storage

BAL was centrifuged at 1500 rpm for 10 minutes to collect the cell pellet. The supernatant was transferred into a separate tube and used for bacteria plating and counting (2.2.1). 500 ul of culture medium (1% Antibiotic-antimycotic, 1% Glutamine, 1% HEPES, 1% β-Mercaptoethanol, 1% Non-essential amino acids, 5% Fetal bovine serum in RPMI medium; sterile filtered, stored at 4°C) was added to the cell pellet, transferred into a cryovial tube (Thermo 368632) and mixed gently by pipette. The suspension was centrifuged at 200 g for 10 minutes and the supernatant was discarded. 250 ul CryoStor CS10 (STEMCELL, 07930) was added to the cell pellet and mixed gently with pipette. Cryovial tubes were placed in a pre-chilled Mr. Frosty container (Nalgene 5100-0001) for 20 min at 4°C. Then the Mr. Frosty container was stored at -80°C and be kept frozen for a maximum of one week.

(2) Thawing process

10 ml of thawing media (20 U/ml of sodium heparin (Sigma H3393), 1:10,000 of 250 U/ul of benzonase (Sigma E1014) in culture media) for every sample in 15 ml conical tubes was warmed in a 37°C water bath. The frozen vials of BAL cells were placed in 37°C water bath without agitation for 3 minutes. Thawed cells were gently mixed with 250 ul of pre-warmed culture media by pipetting up and down and this step was repeated three times until the total volume reaches 1 ml. The suspension was added to the warmed 10 ml of thawing media in the 15 ml

conical tube and mixed by flipping the tube up and down gently. The resuspension was centrifuged at 200 g for 10 minutes at room temperature (RT). The supernatant was decanted and 100 ul of culture media was added and mixed gently by flicking the tube.

(3) Cell Preparation

Single cell suspensions of cells from the BAL were pipetted into 96 well polypropylene plates (Corning 6977A05). Cells were centrifuged at 200g for 5 minutes. To discriminate viable and nonviable cells, cisplatin (Fluidigm – Natural Abundance Platinum, Cat 201064) was used. Cisplatin preferentially enters non-viable cells with compromised plasma membranes and covalently binds to protein inside the cells. Therefore, after data acquisition, cisplatin-bound cells would not be included in the analysis because they are non-viable. 20 ul of cisplatin solution (5 mM stock solution diluted 1:1000 in culture medium) was added to each well and the plate was incubated for 2 minutes at RT. 130 ul of culture medium was then added to the sample to dilute the cisplatin to prevent unspecific binding of cisplatin to viable cells. The plate that contained the cells was then centrifuged at 200g for 5 minutes and then vortexed briefly.

(4) Antibody Application for Surface Staining

Cell staining buffer (CSB) was prepared by mixing 100 mg sodium azide (Sigma 71289), 2.5 g bovine serum albumin, protease-free (Sigma A3059) in 500mL low-barium PBS. It is critical that reagents do not contain barium or other heavy metals because these can interfere with detection of mass channels, thus diminishing sensitivity and damaging the CyTOF instrument. A stock solution of CSB is stored at 4°C.

The cells in each well were then treated with 20 ul of mouse Fc-Block reagent (0.5 mg/ml stock diluted 1:100 in cell staining buffer (CSB); BioLegend 101319) and incubated for 10 minutes at RT. Twenty ul of metal-coupled surface antibody cocktail (1:100 each surface Ab in CSB) was added to each well and incubated for 30 minutes at RT. The cells were then washed with 150 ul of CSB and the plate centrifuged at 200g for 5 minutes.

(5) Cell Stabilization

Cell stabilization is performed to preserve the cells that are stained with metal-coupled surface antibodies for the rest of the CyTOF protocol so that accurate data can be acquired at the end. 100uL of the culture medium was added to each well and the samples were thoroughly and gently mixed by pipetting up and down. 100 uL of 3.2% Paraformaldehyde (1:4 of 16% stock PFA into CyTOF PBS; Fisher 040425) was added to each well and the samples were thoroughly and gently pipetted up and down using a multichannel pippetor. The plate was centrifuged at 200g for 5 minutes.

(6) Barcoding

Barcodng involves covalently labeling individual cell samples with cell-reactive palladium chelators and combinatorial barcodes. The barcoding step enables staining pooled samples with intracellular markers, which eliminates sample-to-sample assay variability. Also, the pooled sample can be run on the CyTOF instrument and the debarcodes are used to recover the identity of individual samples for further analysis[70]. After the cell stabilization step, the cells were permeabilized with 100uL of eBioscience Fix/perm buffer (1:4 in Fix/Perm Diluent; Thermo-Fisher 00-5523-00) for 30 minutes at RT. Permeabilization step was performed to

provide optimal condition for detecting intracellular markers later, which are stained in the later step (2.2.5.7). 100 uL of 1X eBioscience perm buffer was added directly to the cells, which were then centrifuged at 200g for 5 minutes. The cells were washed with 150 uL CyTOF PBS (Gibco 10010-023) and the plate was centrifuged at 200g for 5 minutes. The supernatant was discarded. On ice, 100 uL CyTOF PBS was added to corresponding wells in a separate empty polypropylene plate, labeled as a "transfer plate." 10 uL of BarCode Reagent (BCR) was added to the 100 uL CyTOF PBS in the transfer plate and mixed by pipetting up and down three times. BCR contains Palladium-based chelators that covalently label cell samples with combinatorial barcodes. 90 uL of the mix was transferred to corresponding cell samples and then mixed thoroughly and gently 7 times and incubated for 15 minutes at RT.

The samples were washed twice with 150 ul CSB to dilute excess BCR and the plate was centrifuged at 200g for 5 minutes. After the final wash, all the cells from each well were combined into 1 sample in a 5 ml polypropylene tube. The cells were then centrifuged at 200g for 5 minutes and the supernatant was discarded.

(7) Intracellular Staining

Staining for intracellular targets is done by adding 20 u of intracellular antibody per sample, diluted in eBioscience perm buffer to the pooled sample of cells and incubated for 30 minutes at RT. The cells were then washed with 1 ml eBioscience perm buffer and centrifuged at 200g for 5 minutes. The supernatant was discarded and the cells were resuspended in 1mL of 1.6% PFA for 10 minutes at RT and centrifuged at 200g for 5 minutes. The supernatant was discarded and the cells were resuspended in 1ml CSB. The sample was stored at 4ºC overnight.

(8) Intercalator Application

Thr next day, the sample was centrifuged at 200g for 5 minutes and the supernatant was discarded. 1ml of MaxPar Intercalator-IR (500uM stock solution diluted 1:4000 in CyTOF PBS; Fluidigm 201192B) was added to the sample. The sample was incubated for 20 minutes at RT and then centrifuged at 200g for 5 minutes. The cells were then washed with 1 ml of CSB and centrifuged at 200g for 5 minutes. The cells were washed twice with 1ml of Milli-Q water and centrifuged at 200g for 5 minutes. The cells were resuspended in 500ul of Milli-Q water containing a 1:10 dilution of EQ beads (Fluidigm 201078), which are used for normalization. The normalization step is performed to account for signal variation due to changes in instrument performance and the simultaneous use of beads and cells enables correction of signal fluctuations. The amount of Milli-Q water was adjusted to reach a final cell count of 1×10^6 cells/ml. The cell suspension was transferred through 5mL of filter cap tubes to discard debris.

The sample was then run on a CyTOF-Helios mass cytometer at the Mass Cytometry Core at the Dana-Farber Cancer Institute. The acquired data were then analyzed with Cytobank, a cloud-based platform for the analysis and storage of mass cytometry data (www.cytobank.org).

Statistical analysis

The significance of difference was determined using the Student *t* test. Significance was defined as $P < 0.05$.

2.3 Results

2.3.1 CO enhances bacterial clearance in the lung

4 hours after *S. Aureus* inoculation, the animals were placed in an exposure apparatus as previously described and exposed to CO gas (250ppm, for 1h). A BAL was performed for bacteria counts 5 hours and 24 hours after *S. aureus* inoculation. Bacterial colony forming units (CFU) were significantly lower in the BAL from CO treated mice versus control mice both at 5 hours and 24 hours after bacterial challenge (**Figure 4**).

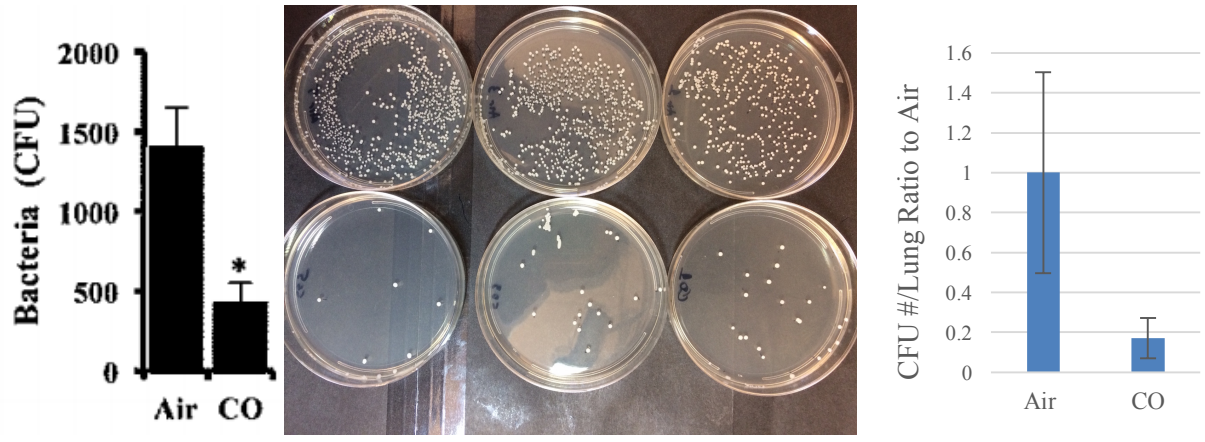

Figure 4. CO enhances bacterial clearance from the lung. (Left) 24 hours after bacterial challenge, *S. aureus* counts are significantly less in BAL from CO-treated mice (lower row) versus BAL from control mice (upper row; N=20 per group; $p<0.01$). (Right) CO also enhances bacterial clearance from the lung 5 hours after bacterial challenge (N=10 per group; $p<0.001$).

2.3.2 Reduction in the number of alveolar macrophages impairs the host's ability to clear bacteria in the lung

Our hypothesis is that CO enhances bacterial killing in the lung, in part by modulating the phenotype of the alveolar macrophage and infiltrating neutrophils. To test whether macrophages were targeted by CO, we depleted alveolar macrophages pharmacologically. We first established the model of alveolar macrophage depletion. 50 ul of clodronate liposomes was determined to be

an optimal dose to deplete the macrophages pharmacologically. Clodronate-liposomes or PBS liposomes were administered twice to CD-1 mice intratracheally for two consecutive days, 24h apart. A BAL was done 24h after the second dose and we observed a significant reduction in macrophage numbers measured in the BAL in clodronate-treated mice vs control. However, a significant amount of neutrophils was detected as well at this time point (**Figure 5**).

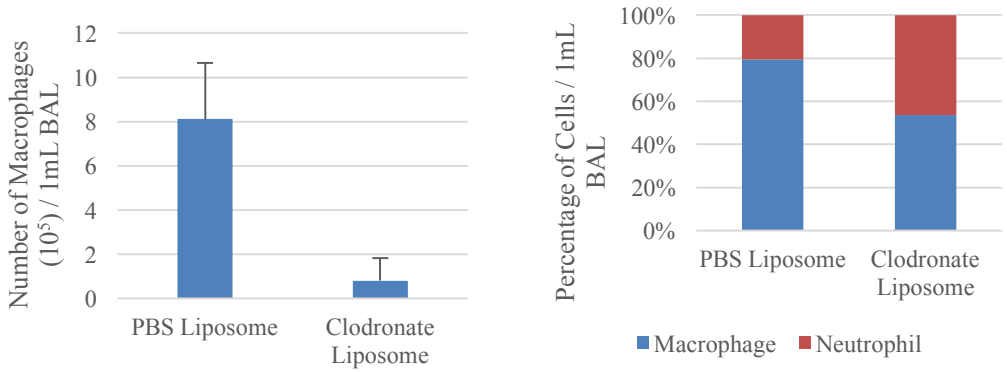

Figure 5. Alveolar macrophage depletion model. The number and percentage of alveolar macrophages in the lung airway after clodronate or PBS-liposomes. The number of alveolar macrophages significantly decreased with clodronate treatment which was accompanied with a significant number of neutrophils (N=3 per group; $p<0.04$).

In order to avoid the contribution of neutrophils we decided to assess the lung airway by BAL, 5 days and 4 days after clodronate administration. Again, the number of alveolar macrophages was significantly decreased with clodronate liposome and at this later time point, neutrophils were not present (**Figure 6**). We moved forward with this model because it reduced the complexity of having neutrophils present.

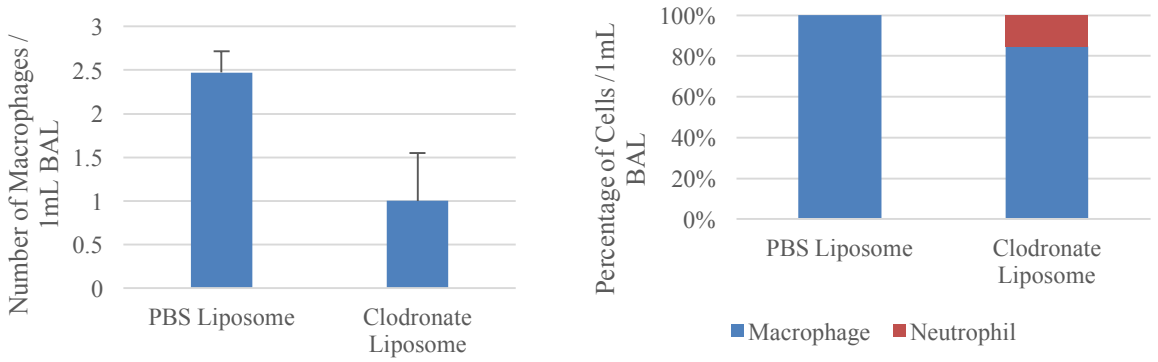

Figure 6. Alveolar macrophage depletion with longer recovery time after liposome administration. Number and percentage of alveolar macrophages in the lung airway after clodronate liposome i.t. injection, given 4 and 5 days before BAL collection. The number of alveolar macrophages significantly dropped with the treatment of clodronate liposome and almost no neutrophils were detected (N=3 per group; $p<0.02$).

To assess whether macrophage depletion impaired the host's ability to clear bacteria in the lung, CD-1 mice were treated with clodronate or PBS liposome 5 and 4 days before *S. aureus*. BAL analysis showed that clodronate treatment reduced the number of alveolar macrophages by approximately 40% and while the bacterial CFU count trended higher in the BAL from the mice treated with clodronate liposome no statistical significance was achieved likely due to the relatively small number of animals in each group (**Figure 7**). Future studies will focus on optimizing this model to be able to determine if the CO-enhanced bacterial clearance as described in Figure 4 is dependent on the resident alveolar macrophage as the cell ultimately responsible for the effects observed with CO.

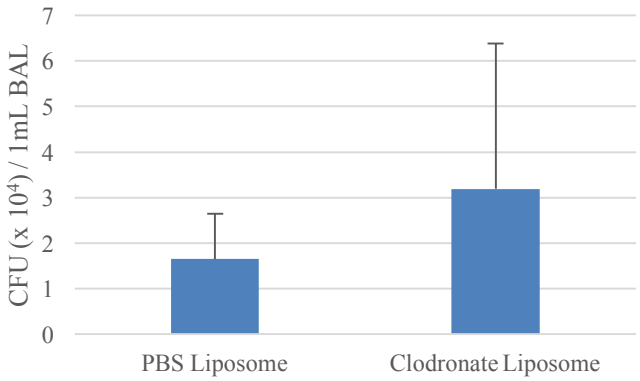

Figure 7. CFU Count in BAL of mice treated with PBS or clodronate liposomes 4 and 5 days before lung infection. BAL was performed 5 hours after lung infection with *S. Aureus* (N=7 per group).

2.3.3 Depletion of neutrophils compromises the hosts ability to clear bacteria in the lung but CO treatment rescues Ly6G-treated mice from lung bacterial infection.

Similar to macrophages we next sought to assess the role of the neutrophil in the CO response. In order to establish the baseline model of neutrophil depletion, the dosage and the time of the treatment of antibodies was first determined. Anti-Ly6G antibody, which is highly selective for neutrophils, was used and compared with a non-specific, antibody isotype control (250ug, i.p.) administered to CD-1 mice 24h before bacterial inoculation. A BAL was performed 5h after inoculation. We observed a significantly greater number of CFU in BAL from Ly6G-treated mice (**Figure 8**) vs control-treated mice supporting a role for the neutrophil in the hosts ability to clear bacteria in the lung. This was not surprising, but was part of the model development to test the effects of CO.

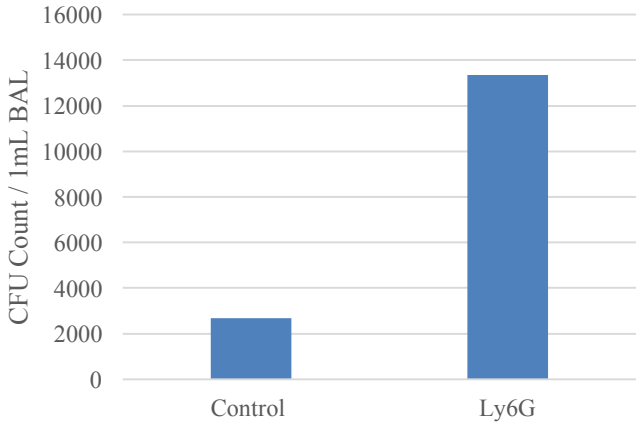

Figure 8. Anti-Ly6G Ab treatment (250ug) and lung bacterial infection. CFU count from BAL of mice treated with Ly6G or isotype 24 hours before lung infection. Note that the CFU count trends higher in Ly6G-treated mice compared to control (N=2 per group).

Twenty-four hours after 250ug or 500ug of anti-Ly6G antibody is given i.p. to CD-1 mice, the number of circulating neutrophils in the whole blood decreased significantly (**Figure 9**).

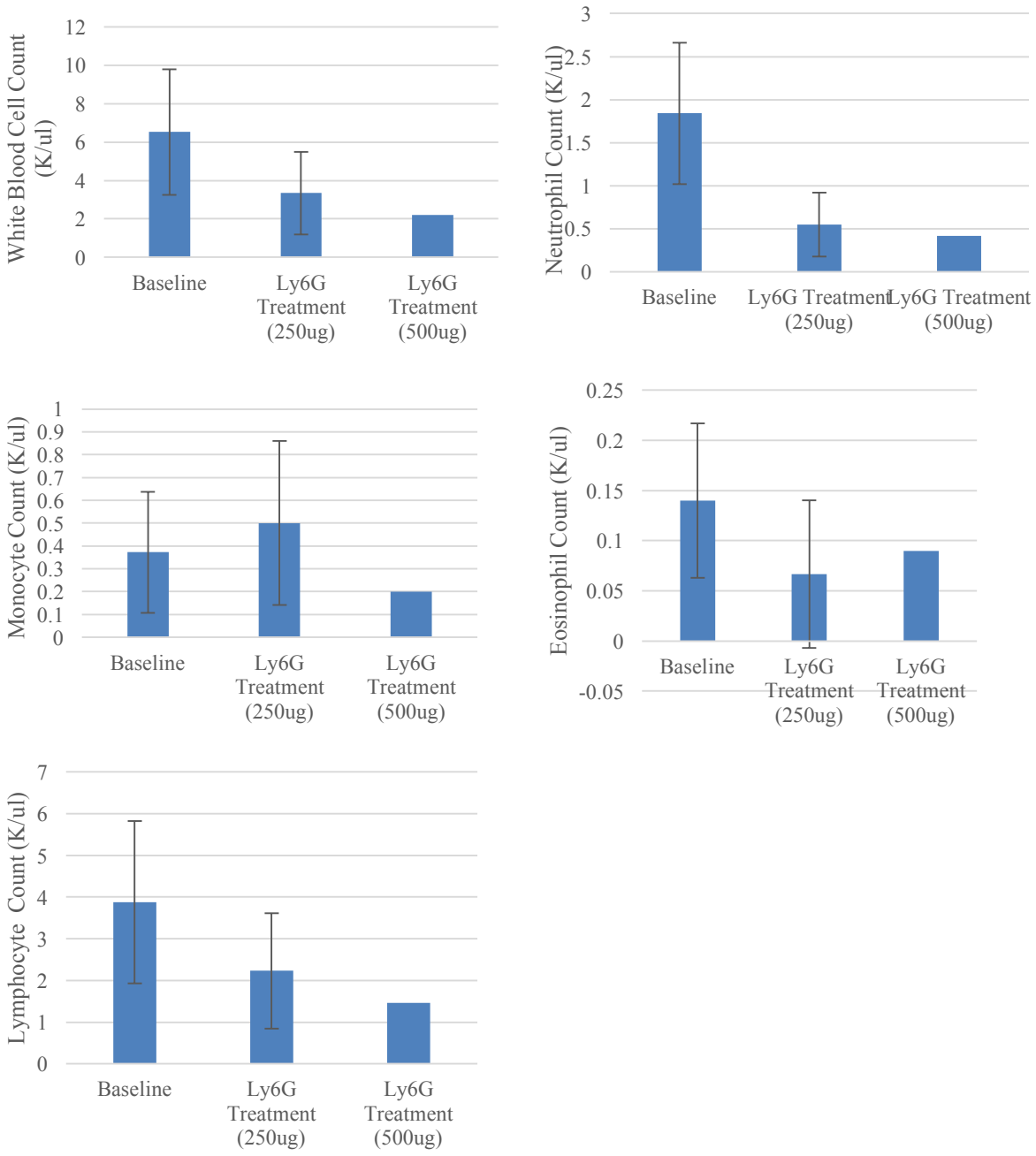

Figure 9. Anti-Ly6G Ab treatment and CBC count. CBC result of the whole blood taken before and 24 hours after anti-Ly6G antibody treatment (250ug and 500ug). The number of neutrophils significantly dropped after anti-Ly6G antibody injection ($p<0.05$). The number of white blood cells and lymphocytes dropped after anti-Ly6G antibody injection but not significantly. The number of monocytes and eosinophils did not change much with anti-Ly6G antibody treatment (N=5 for baseline, N=3 for 250ug Anti-Ly6G Ab treatment, N=2 for 500ug Anti-Ly6G Ab treatment).

To examine the effect of CO in the bacteria infection model in the absence of neutrophils, CD-1 mice were given 250ug of anti-Ly6G antibody or isotype as control, 24 hours before

inoculation with bacteria, and 4h after infection, the mice were treated with air or CO (250 ppm, 1hr). A BAL was performed at the end of the CO exposure. Depletion of neutrophils resulted in higher numbers of bacteria in the airway compared to isotype control. In the anti-Ly6G-treated mice, CO was able to enhance bacterial clearance (**Figure 10**) suggesting an Ly6G+neutrophil-independent response, however, there was a Ly6G- neutrophil population that infiltrated the lung in CO-treated animals. The augmented bacterial clearance by CO in the Ly6G-treated mice is most likely due to the infiltration of a different population of neutrophils into the lung in response to CO, which is not observed in the Ly6G-trated mice exposed to Air (**Figure 10**).

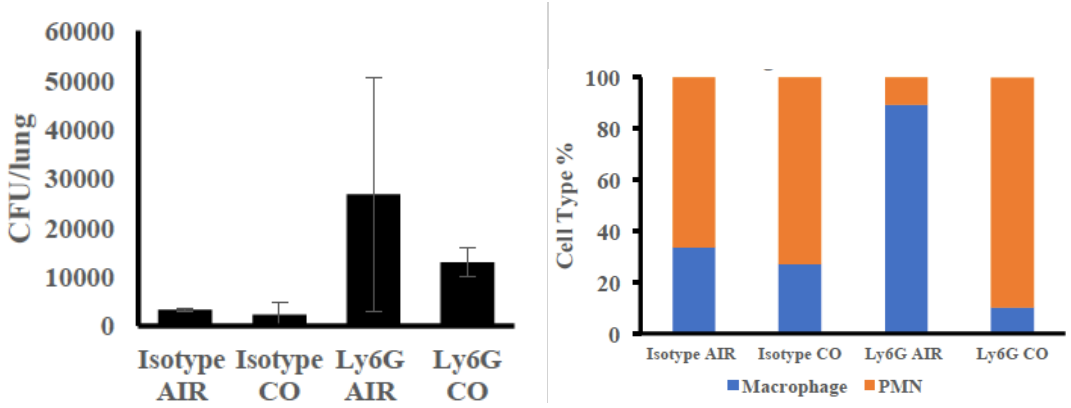

Figure 10. Anti-Ly6G Ab treatment, CO exposure and lung bacterial infection. CFU count and percentage of macrophages and neutrophils in BAL. CD-1 mice were given i.p. injection of isotype or anti-Ly6G antibody 24 hours before bacterial infection in the lung. 4 hours after infection, mice were either treated with CO (250ppm, 1hr) or none. 5 hours after infection, BAL was performed. (Left) Ly6G-treated mice exhibited higher CFU count than isotype-treated mice. CO treatment in Ly6G-treated mice resulted in lower CFU count than Ly6G-treated mice that received no CO treatment. (Right) Ly6G treatment successfully depleted neutrophils in the Ly6G-treated mice ($p<0.0001$). Surprisingly, infiltration of neutrophils was observed in the Ly6G-treated mice that were exposed to CO ($p<0.01$).

2.3.5 CO induces a phenotypic change in alveolar macrophages and recruited neutrophils

Lung airway cells were collected 5 hours after bacterial inoculation with *S. aureus* and processed for CyTOF (See Methods). One group of mice was exposed to CO (250 ppm) for the last hour before BAL and another group received no treatment. The antibodies that were used are

listed in Table I. CyTOF, ViSNE single-cell analysis of CyTOF staining data from lung immune response to bacterial infection was done.

ViSNE plots are generated with Cytobank and plotted as below. Each dot represents a single cell that is analyzed and profiled for selected epitopes (**Table I**) and these dots are distributed on tSNE1 and tSNE2, which are an arbitrary dimension that separates cells based on how phenotypically similar they are to each other. The closer they are to each other, the more phenotypically similar they are.

Distinct populations of macrophages and neutrophils were identified as CD68+ macrophages and Ly6G+ neutrophils (**Figure 11**). General shifts within the populations of the macrophages and neutrophils are noticeable. Importantly, and remarkably, there were significant differences between these two cell phenotypes with only the one-hour exposure to CO.

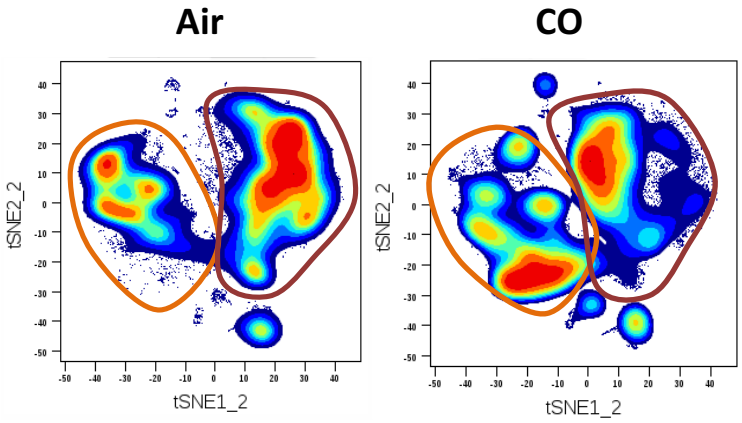

Figure 11. ViSNE plot analysis of CyTOF staining data of lung airway cells exposed to air or CO in *S. Aureus* infection, 5h after inoculation. Populations of macrophages (left cluster) and neutrophils (right cluster) are identified and a general shift within each cell population in the BAL is observed between Air and CO-treated animals.

Further analyses showed smaller populations of cells present including CD4+ T cells, expressing CD3 and CD4, NK cells, expressing NK1.1, CD49b and NKG2D, and eosinophils,

expressing CD11b, F4/80 and Siglec-F. No significant difference in these populations of cells was noted between the air and the CO-treated group.

Expression level of the phenotypic markers (**Table 1**) in airway macrophages and neutrophils is displayed in Figure 12A-C. No significant difference was observed.

Marker	Clone	Metal
EpCAM	G8.8	113In
CD4	RM4-5	115In
CD45	30-F11	141Pr
CD8a	53-6.7	142Nd
CD49b	DX5	143Nd
JAML	4E10	144Nd
NKG2D	191004	145Nd
CD11c	N418	146Nd
PU.1	phpu13	147Sm
Ly6G	1A8	148Nd
CD19	6D5	149Sm
CX3CR1	SA011F11	150Nd
Ly6C	HK1.4	151Eu
CD3	145-2C11	152Sm
CD172a/SIRPa	P84	153Eu
PD-L1	10F.9G2	154Sm
CD68	FA-11	155Gd
CD14	Sa14-2	156Gd
CD205	NLDC-145	158Gd
CD206	C068C2	159Tb
Sca-1	E13-161.7	160Gd
Arginase I	Poly	161Dy
FoxP3	FJK-16s	162Dy
NK1.1	PK136	163Dy
Ki67	16A8	164Dy
CD115	460615	165Ho
CD103	2E7	166Er
SR-AI/MSR	268318	167Er
C-kit	2B8	168Er
CD11b	M1/70	169Tm
Siglec-F	E50-2440	170Er
CD279/PD-1	29F.1A12	171Yb
TCRgd	GL3	172Yb
CD69	H1.2F3	173Yb
CCR2	SA203G11	174Yb
F4/80	BM8	175Lu
GR1-Ly6G/Ly6C	RB6-8C5	176Yb
I-A/I-E	M5/114.15.2	209Bi

Table 1. CyTOF mouse antibody panel. This panel of mouse surface and intracellular markers conjugated with heavy metal isotopes that were used for CyTOF staining.

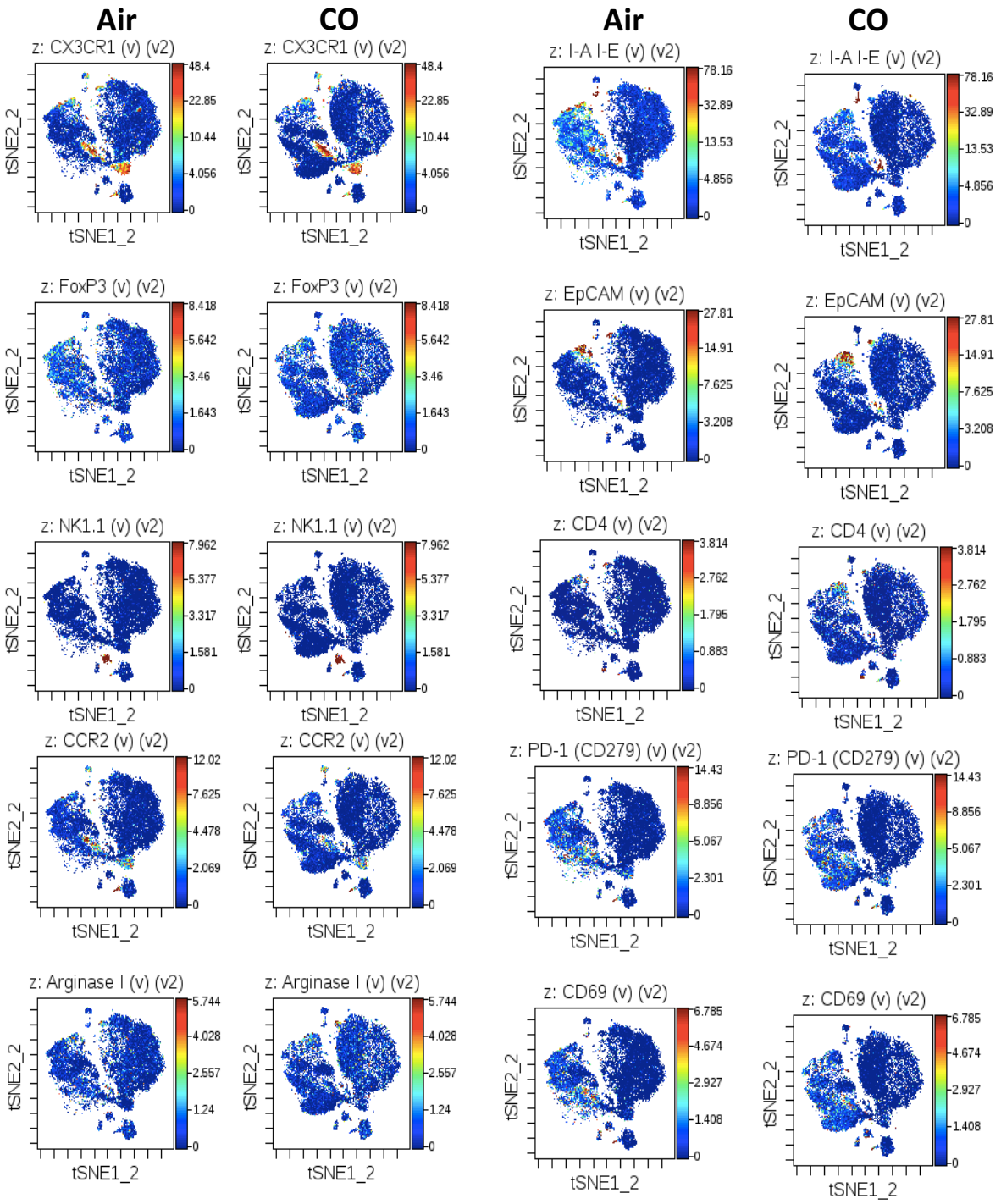

Figure 12A. ViSNE single-cell analysis of CyTOF staining data of lung immune cells exposed to air or CO in bacterial infection. CD-1 mice were exposed to air or CO (250ppm, 1hr) 4 hours after bacterial infection and BAL was done immediately after exposure to CO was complete. Markers of interest include CX3CR1, FoxP3, NK1.1, CCR2, Arginase I, I-A/I-E, EpCAM, CD4, PD-1 and CD69.

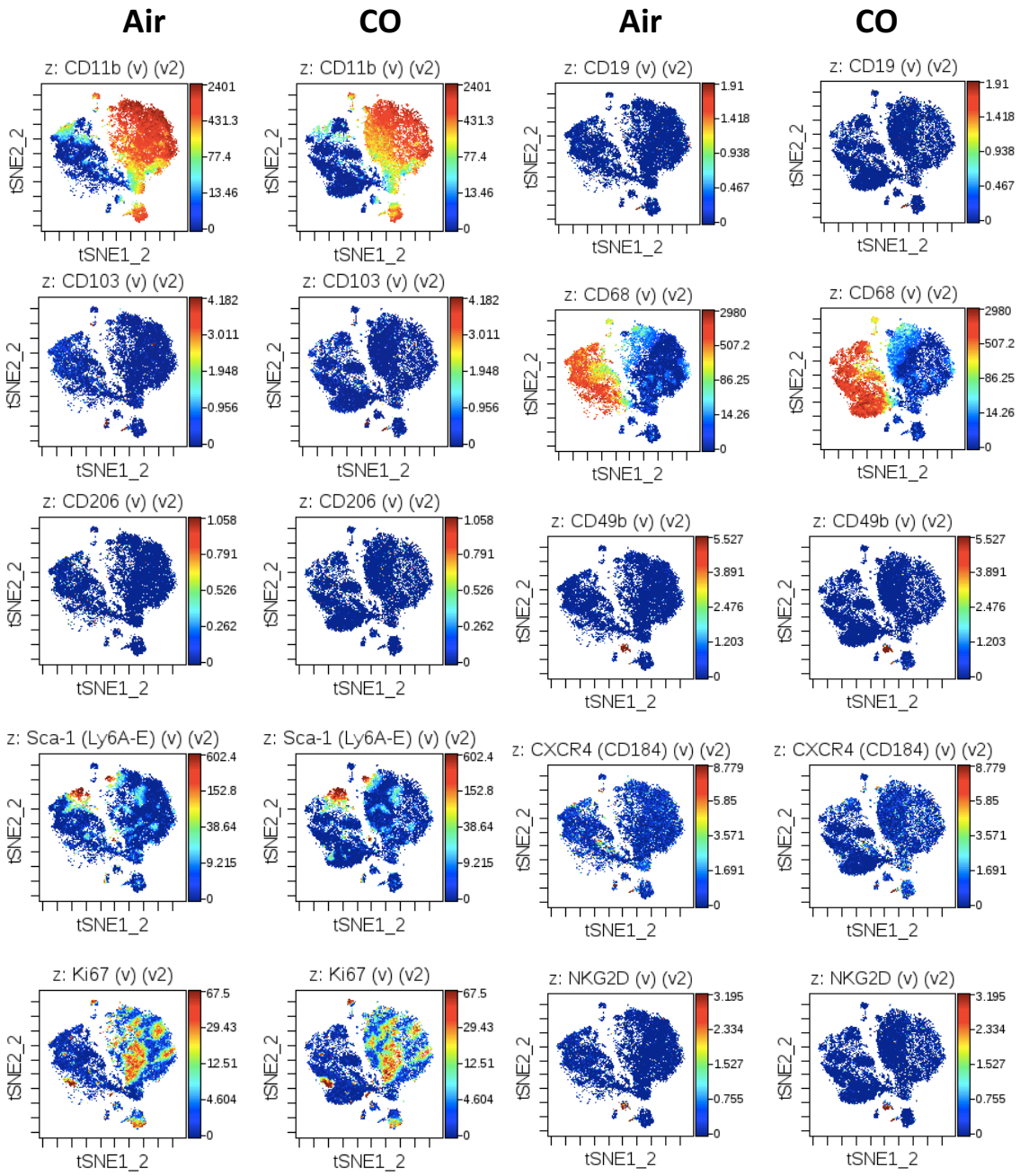

Figure 12B. ViSNE single-cell analysis of CyTOF staining data of lung immune cells harvested from to air or CO-treated mice in response to *S. aureus* as in Figure 6A. Markers of interest include CD11b, CD103, CD206, Sca-1, Ki67, CD19, CD68, CD49b, CXCR4, and NKG2D.

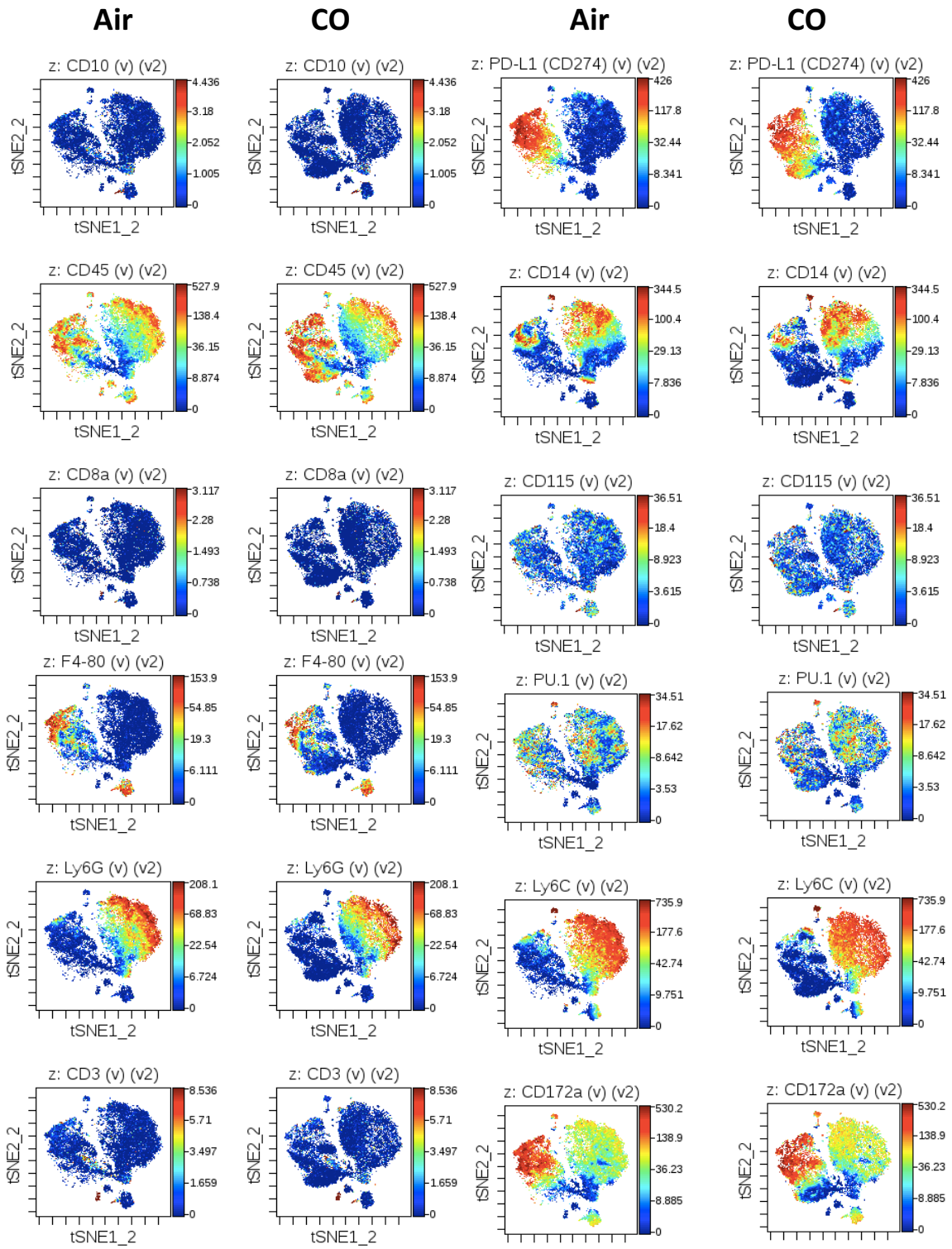

Figure 12C. ViSNE single-cell analysis of CyTOF staining data of lung immune cells in BAL of mice exposed to air or CO + *S. aureus* as in 6A. Markers of interest include CD10, CD45, CD8a, F4-80, Ly6G, CD3, PD-L1, CD14, CD115, PU.1, Ly6C and CD172a.

Within the cluster of neutrophils, the most significant difference noted is the presence of CD68+ neutrophils expressing Ly6C and CD14 in the CO-treated group, which are not present in

the control group (**Figure 13**). Interestingly, CD68 is a macrophage specific marker. Thus these cells seem to be a hybrid of macrophage and neutrophil based on the specific markers being expressed.

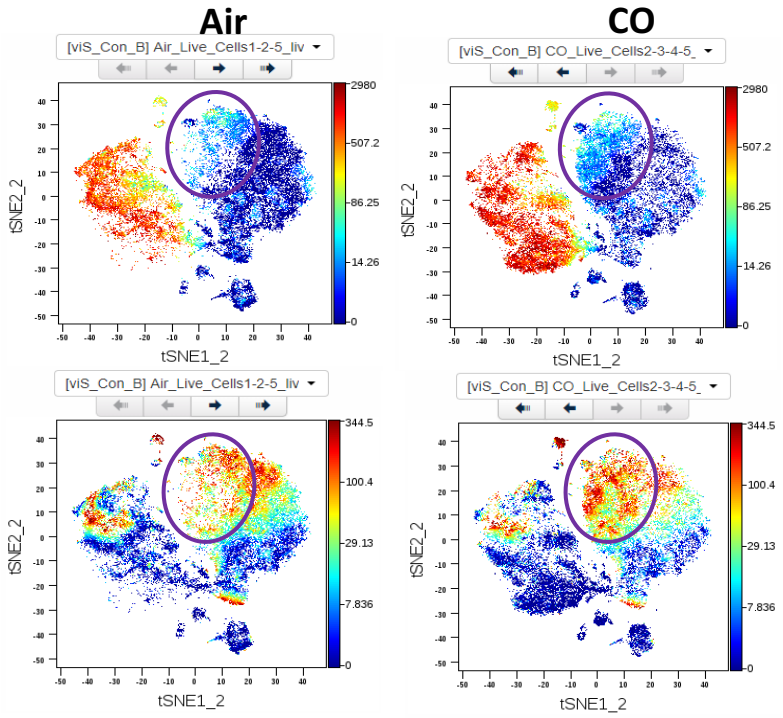

Figure 13. Identification of CD68+ neutrophils in the CO group. BAL from CD-1 mice exposed to CO (250ppm, 1hr) after bacterial infection has CD68+ (top) and CD14+ neutrophils (bottom). This cell population is not seen in the BAL from mice that received no CO treatment.

Striking differences in the cluster of macrophages was also observed between control and the CO-treated infected animals. Specifically, BAL-recovered cells from the CO group had a population of cells that was not present in control. This cluster of cells displayed a high level of expression of CD64 (also known as FcgRI), CD205, CD11c, TLR2, and Siglec-F (**Figure 14**).

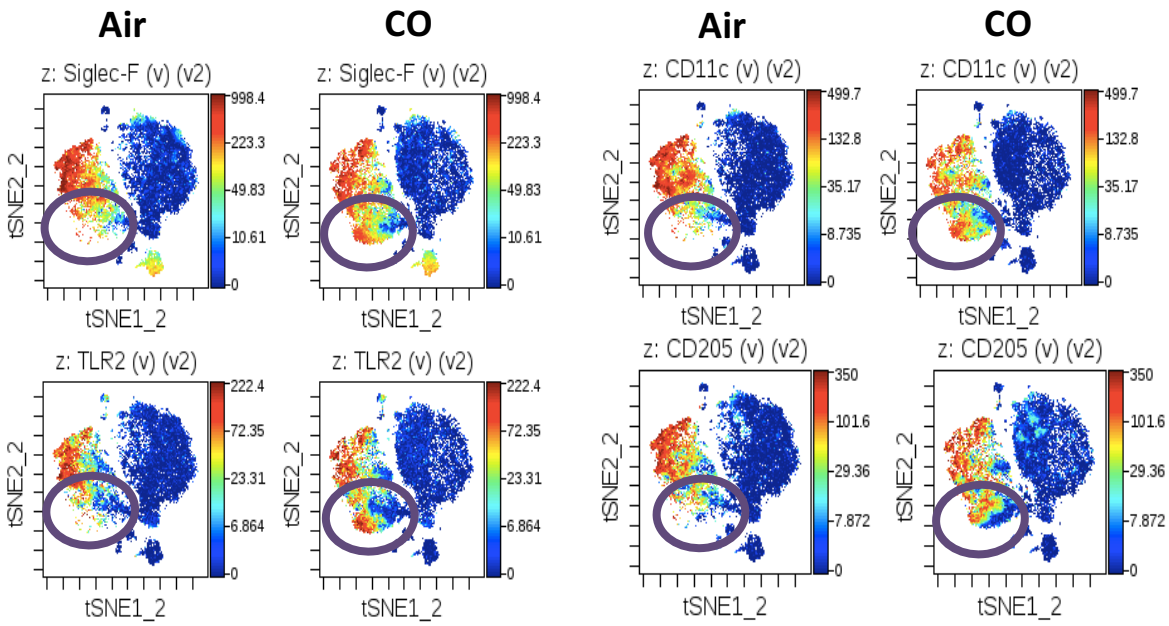

Figure 14. Identification of a subset of macrophages in the CO group. BAL from CD-1 mice exposed to CO (250ppm, 1hr) after bacterial infection has a subpopulation of macrophages that exhibit high expression level of Siglec-F, TLR2, CD11c, and CD205. This cell population is not present in the BAL from air-exposed, infected mice.

Chapter 3: Discussion and Perspectives

3.1 Discussion

Mouse pneumonia model was successfully established. There are different ways of delivering bacteria into the lung airway, such as intranasal inoculation and transtracheal injection. However, our method, which is done by i.t. route, is more efficient, simple, clean and non-invasive compared to other methods for inducing pneumonia in animals. I.t. injection is clean as bacteria can be infused directly into the lung through trachea. This model is also non-invasive because bacteria was successfully delivered into the lung without surgically exposing the trachea. In addition, whether delivery of bacteria was successful or not can be decided immediately after i.t. injection by the animal's increased respiratory rate and a gargling sound from the throat. Therefore, this method puts less stress on the animals.

With this pneumonia model, the effect of CO on the host's ability to clear the bacteria in the lung was tested. 4 hours after bacterial infection, the animals were exposed to CO (250ppm) for an hour and a BAL was performed 24 hours after bacterial infection. Exposing the animals to CO for an hour, 4 hours after infection, significantly enhanced their ability to clear the bacteria in the lung. It is remarkable to note that CO treatment for one hour can drastically enhance the host's response to fight against pathogen.

Previous studies have shown that the therapeutic effect of CO in various animal models is mediated through immune cells. Therefore, in this study, we explored whether CO enhances bacterial clearance by augmenting the immune cells' ability to kill the bacteria.

CyTOF was used to observe phenotypic changes in lung immune cells after CO treatment in a mouse pneumonia model. CyTOF is without a doubt an advanced technology tool that provides the most comprehensive understanding of cell phenotypes and intracellular markers. This technology is far more advanced than flow cytometry, a popular laser-based technology used for marker detection and measurement of expression level. Since flow cytometry takes advantage of fluorescent-labeled antibodies, the number of antibodies and fluorophores that can be used in one single experiment is limited. A typical flow cytometry panel can use 8-12 parameters. On the other hand, in CyTOF, antibodies are conjugated to metal isotopes, which allows us to use far more parameters, typically up to 40 markers simultaneously in a single experiment.

The ViSNE analysis of CyTOF staining data showed that the majority of immune cells in the lung airway were macrophages and neutrophils. In addition, between the air group and the CO group, some remarkable differences were observed in terms of the distribution of cells and the expression level of some markers. As shown in Figure 11, it is remarkable to note that just 1 hour exposure of CO led to a noticeable shift in the populations of macrophages and neutrophils. By assessing the expression level of each marker, we identified a subset of neutrophils in the CO group that express a macrophage specific marker CD6, which is not present in the control. This same population also expressed high level of CD14, which is a co-receptor for the detection of LPS along with TLR4[72]. Little is known about CD68+ neutrophils in literature and the role of CD14 in neutrophils so it is inconclusive to state that this new subset of neutrophils found in the CO group contributes to the effective killing of bacteria. However, CO treatment induced a phenotypic change in neutrophils and led to the emergence of this new cell population, which

warrants further examination. Further investigation into this population of CD68+ neutrophils is needed to assess their bacterial killing ability.

In addition to CD68+ neutrophils, a new population of cells was detected in the cluster of macrophages in the CO group. This subset of macrophages expressed a high level of CD64 and TLR2. CD64, or FcgRI, is known to mediate phagocytosis, antigen presentation, cytokine release and superoxide generation. TLR2, a member of the TLR family, plays a crucial role in pathogen recognition and activation of innate immune responses. High expression level of these markers indicates that this subset of macrophages exhibit augmented bacterial killing properties. Therefore, it can be suggested that CO treatment induces such phenotypic changes in macrophages to be more effective at bacterial killing.

Next, given that macrophages and neutrophils play an important role in innate immune responses to lung infection and that the effect of CO is in part mediated through these cells, we explored whether the lack of either cell type results in the host's compromised ability to kill bacteria and the therapeutic effect of CO in pneumonia. The use of liposome clodronate allowed reduction in numbers of alveolar macrophages. Reduced number of alveolar macrophages was shown 1 and 2 days after clodronate liposome treatment but a significant amount of neutrophils was observed in BAL, most likely to get rid of the debris of macrophages that went through apoptosis. Therefore, to avoid the presence of neutrophils at the time of infection, we collected BAL cells 4 and 5 days after clodronate liposome. The number of alveolar macrophages was lower and no neutrophils were observed. Thus, we chose to give bacteria into the lung 5 days after clodronate liposome treatment. BAL was collected 5 hours after infection and the results

showed that the CFU count trended higher in the clodronate-treated mice versus PBS liposome treated mice, but statistical significance was not observed likely due to a small number of animals. These studies need to be repeated to increase the number of animals/group.

Anti-Ly6G antibody was used to deplete neutrophils. The number of neutrophils in the whole blood after Ly6G antibody treatment dropped significantly, confirming that the antibody successfully depleted neutrophils. In addition, the experiments showed that Ly6G treatment compromised the host's ability to effectively clear the bacteria in the lung, validating the importance of neutrophils in fighting against lung infection. Surprisingly, in Ly6G-treated mice, CO treatment recruited neutrophils into the airway, which should have been depleted by the antibody treatment. Based on the CFU counts, Ly6G-treated mice exposed to CO exhibited lower CFU versus Ly6G-treated mice exposed to air. This enhanced bacterial killing by CO in Ly6G-treated mice is most likely due to these recruited neutrophils and will be the focus of future studies. Given the CyTOF data, we conclude that CO by some mechanisms of action, alters the immune response specifically to augment bacterial clearance and likely is dictating how the cells are phenotypically altered to maximize the efforts to clear the pathogen.

3.2 Limitations and Future Direction

In this study, CyTOF allowed us to picture phenotypic changes caused by CO exposure on lung immune cells. However, one limitation of CyTOF is that it does not provide functional analysis of the cells. It can only identify the cell types by their surface marker expression. In other words, even though new cell populations were identified in the BAL exposed to CO, how these cells contribute to effective bacterial clearance cannot be explained based on CyTOF staining data alone. Therefore, based on the data generated from CyTOF profiling, our next experiments must be designed to gain an understanding of how these phenotypically modified cells function to kill bacterial. Whether this is unique to lung infection is also a question we can answer by utilizing and comparing with our peritoneal infection model.

Using clodronate liposomes was a technical challenge and while we followed the vast literature knowledge, it was not as straight forward as we had anticipated. Ultimately, it may not have been the most efficient way to study the effect of macrophage depletion on lung bacterial clearance and therapeutic effects of CO in this context. Even though the number of alveolar macrophages was reduced, clodronate liposomes failed to completely deplete this population and in fact may have resulted in recruitment of macrophage-like cells, e.g. monocytes due to the death of the resident alveolar cells. In addition, neutrophils could have been compensating for the lack of alveolar macrophages to fight against pathogens. There are different factors to consider in this model, which may have resulted in variable CFU counts. Therefore, future studies will involve repeating this experiment to increase the animal number and to confirm that reduction in the number of alveolar macrophages results in the host's weakened ability to clear the bacteria.

An alternative method to deplete alveolar macrophages is the use of CD11c diphtheria toxin receptor (DTR) mice, which express DTR under control of the full CD11c promoter. When diphtheria toxin is delivered into the lung, it can specifically deplete local CD11c+ cells or alveolar macrophages. Mouse cells do not express a native DT receptor, thus the genetically altered CD11c cells have been engineered to express the receptor thus making them sensitive to DT. Roberts et al. has successfully depleted alveolar macrophages in this manner[73] and this method may provide us a better understanding of the role of alveolar macrophages in bacterial lung infection and how the effect of CO would be mediated in this setting.

Results from the neutrophil depletion with CO treatment were interesting and warrants further investigation. We clearly show that that lack of neutrophils results in the host's compromised immune response to infection, which is in line with what is known about the innate immune system and the role of the neutrophil. It was surprising that CO treatment somehow recruited neutrophils into the lung airway in an otherwise neutrophil-depleted animal, which should have been depleted by the well characterized anti-Ly6G Ab. Future studies will be designed to profile the phenotypes of these cells, possibly by using CyTOF technology. This set of data has a significant implication for CO as a potential therapeutic agent in clinical setting as CO treatment can likely mobilize and recruit neutrophils to an injured site in individuals whose immune system has been compromised and suffers from neutropenia. Therefore, more repeats of this experiment will be performed to dissect in detail how CO triggers release and recruitment of neutrophils into the airway.

One problem our lab encountered in this project is the host's varying response to lung infection seemingly on a seasonal basis. Reproducibility of the data has been a challenging aspect of this project as the mice exhibited more tolerance to bacterial infection as well as different response to anti-Ly6G antibody treatment during fall and winter. This challenge reflects the complexity of the immune system in mice and suggests that there are multitudes of other factors such as circadian rhythms involved in defense against bacterial infection in the lung that remain unclear.

In summary, this work showed that CO is a potent immunomodulatory molecule which has now been accepted after 20 years of research. CO is currently in multiple clinical trials as an inhaled gas for lung disease including pulmonary fibrosis and respiratory distress syndrome. Additionally, a CO-saturated hemoglobin solution has been formulated to treat sickle cell disease and prevent rejection of a transplanted organ. The data generated here will contribute to an ever-increasing body of literature that will contribute to one day having this simple gas in the armamentarium of clinical tools to treat disease and alleviate human suffering.

4. Bibliography

(1) Douglas, C. G., Haldane, J. S. & Haldane, J. B. The laws of combination of haemoglobin with carbon monoxide and oxygen. *J. Physiol.* 44, 275–304 (1912)
(2) Rose, J. J. *et al*. Carbon Monoxide Poisoning: Pathogenesis, Management, and Future Directions of Therapy. *Am. J. Respr. Crit. Care. Med.*195, 596-606 (2017)
(3) Motterlini, R. and Otterbein, L.E. The therapeutic potential of carbon monoxide. *Nat. Rev. Drug Discov.* 9, 728–743 (2010)
(4) Zuckerbraun, B. S. *et al.* Carbon monoxide signals via inhibition of cytochrome c oxidase and generation of mitochondrial reactive oxygen species. *FASEB J.* 21, 1099-106 (2007)
(5) Tenhunen, R., Marver, H. S. & Schmid, R. The enzymatic conversion of haem to bilirubin by microsomal haem oxygenase. *Proc. Natl Acad. Sci.* USA 61, 748–755 (1968)
(6) Choi, A. M. Heme oxygenase-1 protects the heart. *Circ Res*. 89, 105-7 (2001)
(7) Zarjou, A. *et al*. Proximal tubule H-ferritin mediates iron trafficking in acute kidney injury. *J. Clin. Invest.* 123, 4423-4434 (2013)
(8) Rodwell, V. W., Bender, D. A., Botham, K. M., Kennelly, P. J. Weil, P. A. Harper's Illustrated Biochemistry. The McGraw-Hill Education (2015)
(9) Delaby, C. *et al.* Subcellular localization of iron and heme metabolism related proteins at early stages of erythrophagocytosis. *PLoS ONE*. 7, e42199 (2012)
(10) Korolnek, T., Hamza, I. Like iron in the blood of the people: the requirement for heme trafficking in iron metabolism. *Front. Pharmacol.* 5, 1-13 (2014)
(11) Ryter, S. W., Alam, J. & Choi, A. M. Haem oxygenase-1/carbon monoxide: from basic science to therapeutic applications. *Physiol*. *Rev*. 86, 583–650 (2006)
(12) Soares, M.P. *et al*. Heme oxygenase-1, a protective gene that prevents the rejection of transplanted organs. *Immunol. Rev.* 184, 275– 285 (2001)
(13) Soares, M.P. *et al.* Expression of heme oxygenase-1 can determine cardiac xenograft survival. *Nat. Med.* 4, 1073–1077 (1998)
(14) Yamashita, K. *et al*. Heme oxygenase-1 is essential for and promotes tolerance to transplanted organs. *FASEB J.* 20, 776–778 (2006)
(15) Otterbein, L. E. *et al.* Exogenous administration of haem oxygenase-1by gene transfer provides protection against hyperoxia-induced lung injury. *J. Clin. Invest.* 103, 1047–1054 (1999)
(16) Kapturczak, M. H. *et al.* Heme oxygenase-1 modulates early inflammatory responses: evidence from the heme oxygenase-1-deficient mouse. *Am. J. Pathol*. 168, 714 (2006)
(17) Yachie, A., *et al*. Oxidative stress causes enhanced endothelial cell injury in human heme oxygenase-1 deficiency. *J. Clin. Invest.* 103, 129-135 (1999)
(18) Dutra, F. F. & Bozza, M.T. Heme on innate immunity and inflammation. *Front. Pharmacol.* 5, 115 (2014)
(19) Belcher, J. D., Nath, K. A. & Vercellotti, G. M. Vasculotoxic and proinflammatory effects of plasma heme: cell signaling and cytoprotective responses. *ISRN Oxidative Med.* (2013)
(20) Yamada, N. *et al*. Microsatellite polymorphism in the heme oxygenase-1 gene promoter is associated with susceptibility to emphysema. *Am. J. Hum. Genet.* 66, 187-195 (2000)

(21) Rueda, B. *et al.* HO-1 promoter polymorphism associated with rheumatoid arthritis. *Arthritis. Rheum.* 56, 3953-8 (2007)
(22) Pechlaner, R. *et al.* Heme oxygenase-1 gene promoter microsatellite polymorphism is associated with progressive atherosclerosis and incident cardiovascular disease. *Arterioscler. Thromb. Vasc. Biol.* 35, 229-36 (2015)
(23) Wegiel, B., Hanto, D. W., Otterbein, L. E. The social network of carbon monoxide in medicine. *Trends. Mol. Med.* 19, 3-11 (2013)
(24) Ferris, C.D. *et al*. Haem oxygenase-1 prevents cell death by regulating cellular iron. *Nat. Cell. Biol.*1, 152-157 (1999)
(25) Balla, G. *et al*. Ferritin: a cytoprotective antioxidant stratagem of endothelium. *J. Biol. Chem.* 267, 18148-18153 (1992)
(26) Jansen, T. & Daiber, A. Direct antioxidant properties of bilirubin and biliverdin. Is there a role for biliverdin reductase? *Front. Pharmacol.* 3, 30 (2012)
(27) Stocker, R. K. *et al.* Bilirubin is an antioxidant of possible physiological importance. *Science*. 235, 1043-6 (1987)
(28) Sarady-Andrews, J.K. *et al.* Biliverdin administration protects against endotoxin-induced acute lung injury in rats. *Am. J. Physiol. Lung Cell. Mol. Physiol.* 289, L1131–L1137 (2005)
(29) Ollinger, R. *et al.* Bilirubin and biliverdin treatment of atherosclerotic diseases. *Cell Cycle* 6, 39–43 (2007).
(30) Ollinger, R. *et al.* Therapeutic applications of bilirubin and biliverdin in transplantation. *Antioxid. Redox Signal.* 9, 2175–2185 (2007).
(31) Vachharajani, T. J., Work, J., Issekutz, A. C. & Granger, D. N. Heme oxygenase modulates selectin expression in different regional vascular beds. *Am. J. Physiol. Heart. Circ. Physiol.* 278, H1613-7 (2000)
(32) Fondevila, C. *et al.* Biliverdin therapy protects rat livers from ischemia and reperfusion injury. *Hepatology*. 40, 1333-41 (2004)
(33) Wegiel, B. *et al.* Biliverdin inhibits Toll-like receptor-4 (TLR4) expression through nitric oxide-dependent nuclear translocation of biliverdin reductase. *Proc. Natl. Acad. Sci. U.S.A.* 108, 18849–18854 (2011)
(34) Wegiel, B. *et al.* Cell surface biliverdin reductase mediates biliverdin-induced anti-inflammatory effects via phosphatidylinositol 3-kinase and Akt. *J. Biol. Chem*. 284, 21369–21378 (2009)
(35) Chen, B. *et al.* Carbon monoxide rescues heme oxygenase-1- deficient mice from arterial thrombosis in allogeneic aortic transplantation. *Am. J. Pathol.* 175, 422–429 (2009).
(36) Sato, K. *et al.* Carbon monoxide generated by heme oxygenase-1 suppresses the rejection of mouse-to-rat cardiac transplants. *J. Immunol.* 166, 4185–4194 (2001).
(37) Hanto, D.W. *et al.* Intraoperative administration of inhaled carbon monoxide reduces delayed graft function in kidney allografts in swine. *Am. J. Transplant.* 10, 2421–2430 (2010)
(38) Sahara, H. *et al.* Carbon monoxide reduces pulmonary ischemia–reperfusion injury in miniature swine. *J. Thorac. Cardiovasc. Surg.* 139, 1594–1601 (2010)
(39) Sarady, J. K. *et al.* Carbon monoxide protection against endotoxic shock involves reciprocal effects on iNOS in the lung and liver. *FASEB J.* 18, 854–856 (2004)

(40) Zuckerbraun, B. S. *et al*. Carbon monoxide prevents multiple organ injury in a model of hemorrhagic shock and resuscitation. *Shock* 23, 527–532 (2005).
(41) Mazzola, S. *et al*. Carbon monoxide pretreatment prevents respiratory derangement and ameliorates hyperacute endotoxic shock in pigs. *FASEB J.* 19, 2045–2047 (2005)
(42) Wegiel, B. *et al.* Nitric oxide-dependent bone marrow progenitor mobilization by carbon monoxide enhances endothelial repair after vascular injury. *Circulation* 121, 537–548 (2010)
(43) Otterbein, L.E. *et al.* Carbon monoxide suppresses arteriosclerotic lesions associated with chronic graft rejection and with balloon injury. *Nat. Med.* 9, 183–190 (2003)
(44) Raman, K. G. et al. Inhaled carbon monoxide inhibits intimal hyperplasia and provides added benefit with nitric oxide. *J. Vasc. Surg*. 44, 151–158 (2006)
(45) Pamplona, A. *et al*. Haem oxygenase-1 and carbon monoxide suppress the pathogenesis of experimental cerebral malaria. *Nature Med.* 13, 703–710 (2007)
(46) Tsoyi, K. *et al.* Haem-oxygenase-1 induction and carbon monoxide-releasing molecule inhibit lipopolysaccharide (LPS)-induced high-mobility group Box 1 release in vitro and improve survival of mice in LPS- and cecal ligation and puncture-induced sepsis model in vivo. *Mol. Pharmacol.* 76, 173–182 (2009)
(47) Lancel, S. *et al.* Carbon monoxide rescues mice from lethal sepsis by supporting mitochondrial energetic metabolism and activating mitochondrial biogenesis. *J. Pharmacol. Exp. Ther.* 1329, 641–648 (2009)
(48) Chung, S. W., Liu, X., Macias, A. A., Baron, R. M. & Perrella, M. A. Haem oxygenase-1-derived carbon monoxide enhances the host defense response to microbial sepsis in mice. *J. Clin. Invest.* 118, 239–247 (2008)
(49) Bathoorn, E. *et al.* Anti-inflammatory effects of inhaled carbon monoxide in patients with COPD: a pilot study. *Eur. Respir. J.* 30, 1131–1137 (2007)
(50) Otterbein, L. E., Mantell, L. L. & Choi, A. M. Carbon monoxide provides protection against hyperoxic lung injury. *Am. J. Physiol.* 276, L688–L694 (1999)
(51) Cepinskas, G., Katada, K., Bihari, A. & Potter, R. F. Carbon monoxide liberated from carbon monoxidereleasing molecule CORM-2 attenuates inflammation in the liver of septic mice. *Am. J. Physiol. Gastrointest. Liver Physiol.* 294, G184–G191 (2008)
(52) Ott, M. C. *et al*. Inhalation of carbon monoxide prevents liver injury and inflammation following hind limb ischemia/reperfusion. *FASEB J*. 19, 106–108 (2005)
(53) Foresti, R. et al. Vasoactive properties of CORM-3, a novel water-soluble carbon monoxide-releasing molecule. Br. J. Pharmacol. 142, 453–460 (2004)
(54) Motterlini, R. et al. CORM-A1: a new pharmacologically active carbon monoxide-releasing molecule. FASEB J. 19, 284–286 (2005)
(55) Belcher, J. D. *et al*. MP4CO, a pegylated hemoglobin saturated with carbon monoxide, is a modulator of HO-1, inflammation, and vaso-occlusion in transgenic sickle mice. *Blood*. 122, 2757-64 (2013)
(56) Nakao, A. *et al.* Ex vivo application of carbon monoxide in University of Wisconsion solution to prevent intestinal cold ischemia/reperfusion injury. *Am. J. Transplant.* 6, 2243-55 (2006)

(57) Berberat, P. O. *et al.* Heavy chain ferritin acts as an antiapoptotic gene that protects livers from ischemia reperfusion injury. *FASEB J.* 17, 1724-6 (2003)

(58) Bilban, M. *et al.* Carbon monoxide orchestrates a protective response through PPARγ. *Immunity* 24, 601–610 (2006)

(59) Chin, B.Y. *et al.* Hypoxia-inducible factor 1a stabilization by carbon monoxide results in cytoprotective preconditioning. *Proc. Natl. Acad. Sci. U.S.A.* 104, 5109–5114 (2007)

(60) Sawle, P. *et al.* Carbon monoxide-releasing molecules (CO-RMs) attenuate the inflammatory response elicited by lipopolysaccharide in RAW264.7 murine macrophages. *Br. J. Pharmacol*. 145, 800–810 (2005)

(61) Wegiel, B. et al. Nitric oxide-dependent bone marrow progenitor mobilization by carbon monoxide enhances endothelial repair after vascular injury. Circulation 121, 537–548 (2010)

(62) Otterbein, L.E. et al. Carbon monoxide suppresses arteriosclerotic lesions associated with chronic graft rejection and with balloon injury. Nat. Med. 9, 183–190 (2003)

(63) Fondevila, C. *et al.* Biliverdin therapy protects rat livers from ischemia and reperfusion injury. *Hepatology*. 40, 1333-41 (2004)

(64) Song, R. *et al.* Carbon monoxide promotes Fas/CD95-induced apoptosis in Jurkat cells. *J. Biol. Chem.* 279, 44327–44334 (2004)

(65) Wegiel, B. *et al*. Macrophages sense and kill bacteria through carbon monoxide-dependent inflammasome activation. *J. Clin. Invest.* 124, 4926-40 (2014)

(66) The top 10 causes of death. Geneva: World Health Organization, 2013 (http:// www.who.int/mediacentre/factsheets/ fs310/en/index.html)

(67) Eddens, T., Kolls, J. K. Host defenses against bacterial lower respiratory tract infection. *Curr. Opin. Immunol.* 24, 424-430 (2012)

(68) Martin, T. R. & Frevert, C. W. Innate immunity in the lungs. *Proc. Am. Thora. Soc.* 2, 403-411 (2005)

(69) Finisguerra, V. *et al.* MET is required for the recruitment of anti-tumoural neutrophils. *Nature*. 522: 349-53 (2015)

(70) Zunder E. R. *et al*. Palladium-based mass tag cell barcoding with a doublet-filtering scheme and single-cell deconvolution algorithm. *Nat. Protoc.* 12, 316-33 (2015)

(71) Amir, E. *et al*. viSNE enables visualization of high dimensional single-cell data and reveals phenotypic heterogeneity of leukemia. *Nat. Biotechnol.* 31, 545-552 (2013)

(72) Kitchens, R. L. Role of CD14 in cellular recognition of bacterial lipopolysaccharides. *Chem. Immunol.* 74, 61-82 (2000)

(73) Roberts, L. M., *et al.* Depletion of alveolar macrophages in CD11c diphtheria toxin receptor mice produces an inflammatory response. *Immun. Inflamm. Dis.* 3, 71-81 (2015)